Beetsma, Roel; Cimadomo, Jacopo; Van Spronsen, Josha

Working Paper

One scheme fits all: A central fiscal capacity for the EMU targeting eurozone, national and regional shocks

ECB Working Paper, No. 2666

Provided in Cooperation with:
European Central Bank (ECB)

Suggested Citation: Beetsma, Roel; Cimadomo, Jacopo; Van Spronsen, Josha (2022) : One scheme fits all: A central fiscal capacity for the EMU targeting eurozone, national and regional shocks, ECB Working Paper, No. 2666, ISBN 978-92-899-5115-9, European Central Bank (ECB), Frankfurt a. M., https://doi.org/10.2866/103730

This Version is available at:
https://hdl.handle.net/10419/264492

EUROPEAN CENTRAL BANK
EUROSYSTEM

Working Paper Series

Fabio Franch, Luca Nocciola, Angelos Vouldis

Temporal networks in the analysis of financial contagion

No 2667 / June 2022

Abstract

This paper studies the dynamics of contagion across the banking, insurance and shadow banking sectors of 16 advanced economies in the period 2006-2018. We construct Granger causality-in-risk networks and introduce higher-order aggregate networks and temporal node centralities in an economic setting to capture non-Markovian network features. Our approach uncovers the dynamics of financial contagion as it is transmitted across segments of the financial system and jurisdictions. Temporal centralities identify countries in distress as the nodes through which contagion propagates. Moreover, the banking system emerges as the primary source and transmitter of stress while banks and shadow banks are highly interconnected. The insurance sector is found to contribute less to stress transmission in all periods, except during the global financial crisis. Our approach, as opposed to one that uses memoryless measures of network centrality, is able to identify more clearly the nodes that are critical for the transmission of financial contagion.

Keywords: Financial networks, Granger causality-in-tail, GARCH, non-Markovian, systemic risk

JEL classification: C02, C22, G01, G2

Non technical summary

The interconnectedness of the financial system does not only imply beneficial diversification but could also operate as an amplification channel when the initial shock is sufficiently strong, with severe consequences on the macroeconomy. This has been illustrated often during the financial contagion episodes of the last decade, involving banks, shadow banks and insurance firms.

In this paper we empirically investigate the patterns of cross-sectoral contagion for the period starting just before the global financial crisis, in 2006, and up to 2018. We study the main segments of the financial system for 16 advanced economies, namely banks, insurance firms and shadow banks. Our aim is to identify the role played by the various financial segments in the crisis propagation, i.e. whether they act as sources, transmitters or receivers of financial stress. We apply a methodology that captures the dynamic evolution of contagion across time and multiple country-sector pairs, rather than focusing only on bilateral transmission.

We utilise recently introduced mathematical tools for the study of dynamic networks, i.e. networks with time-varying topologies. Nodes in our networks represent country-sector pairs (e.g. US banks) while links correspond to incremental predictive power concerning the realisation of tail risk within a time window, which is interpreted as direct transmission of risk. We identify indirect contagion, i.e. stress transmission intermediated by other nodes in the system, by considering time-respecting contagion paths that represent transmission chains across time. A time scale parameter determines the range of transmission channels encompassed by our methodology, e.g. to include also channels involving volume adjustment (e.g. credit crunches) which are more slowly moving compared to price adjustments (e.g. yield increases).

Our analysis points to the tight interconnectedness of the banking and shadow banking sectors during contagion episodes and the relatively lower systemic risk posed by the insurance sector. Overall, the average crisis event starts either from the banking or the shadow banking sector, while insurers are sometimes affected at a later stage. Banking sectors seem to play the most crucial role in the amplification of financial contagion, compared to both insurance firms and shadow banks. The insurance sector acts as a receiver of stress during the early and the later phase of the global financial crisis.

1 Introduction

The global financial crisis of 2007-2009 and its subsequent transformation into a European crisis represents a stark example of how financial contagion can be transmitted within the international financial system. The cross-border and cross-sectoral dimensions feature prominently in the transmission of this financial crisis as well as other past ones. These transmission channels illustrate vividly that interconnectedness does not only imply beneficial loss-absorbing diversification, but could also operate as an amplification channel when the initial shock is sufficiently strong, with severe macroeconomic consequences (Acemoglu et al. (2015)).[1]

In this paper we empirically investigate the direction of cross-border, cross-sectoral financial contagion for 16 advanced economies during the period 2006-2018. We study the main segments of the financial systems, namely banks, insurance firms and shadow banks. Specifically, we aim to answer the following questions. Which type of financial firms act as the main transmitters of financial contagion, when also international spillovers are considered? Which of them are more likely to be receivers of financial stress? Which patterns of financial contagion most often appear, i.e. which type of financial entities are first impacted when risk materialises and which ones follow? Do these patterns change over time? Do cross-border and cross-sectoral contagion channels operate more strongly during crisis episodes?

The existing literature has adopted concepts from network theory to address such questions on financial contagion. In these networks nodes represent banks, firms, financial instruments or country-level aggregates, and links correspond to various types of connections, either direct or indirect. However, the tools used so far to analyse these networks have limitations. Existing studies typically calculate centrality metrics based on individual network topologies and infer the dynamics of risk transmission at a second stage by analysing the evolution over time of these

[1]The timeline of events that have unfolded during more than a decade exemplifies the cross-border and cross-sector character of financial contagion. After the liquidity crisis experienced by shadow banking entities sponsored, among others, by the French bank BNP Paribas and the German bank IKB in August 2007, the UK bank Northern Rock became the first high-profile default of the global financial crisis in September 2007 (Shin (2009)). The subsequent collapse of the US-based shadow banking institution Lehman Brothers on 15 September 2008 spilled over to money market funds who held short-dated Lehman debt. Lehman's default also triggered a run on the US insurance company AIG, which was bailed out also because of potential spillovers to a number of US and European banks (McDonald and Paulson (2015)).

Furthermore, the spillover of the crisis to Europe led to insolvencies and rescue packages to support banks in distressed countries such as Greece, Ireland, Portugal, Cyprus, Spain. However, banks in other countries without sovereign financing constraints also faced solvency problems, such as the Belgian-French bank Dexia in 2011 (de Groen (2011)) and a number of German institutions. Italian banks also came under pressure during the subsequent years, mostly due to their large amounts of non-performing loans and political uncertainty, while shadow banking entities, such as investment funds, faced valuation losses and were forced to suspend redemptions (e.g. in Luxembourg, see Gorbanyov and Tressel (2016)). Overall, financial turbulence has often reappeared during the last years in various countries and segments of the financial system.

metrics. Another approach has been to aggregate network topologies across time and derive one single topology that stacks all edges that have appeared within the considered time interval. This aggregated network is then analysed to identify the nodes that have played the most critical role. Both these approaches, however, fail to highlight the role played by the network nodes within a time series of interrelated topologies; as a result, the approaches described above may miss critical information contained in these time series.

Figure 1 illustrates this missing information. First, case 1 shows that when each network snapshot is analysed separately, a node that acts as a transmitter may erroneously appear to be either a source or an end-receiver of risk. Case 2 shows that when the aggregate network is analysed (by summing all existing edges that have occurred at some point in time, possibly weighted by their relative number of occurrences), a source node can erroneously be mis-characterised as a transmitter. In that case, the green node was first hit by a shock due to its connection with the blue node on its left and consequently propagated this effect to the blue node on its right. According to the aggregated network, the orange node appears to have had a very similar role, however, this is misleading in that in reality, the only similarity was that the orange node was hit by a shock at time t from the blue node on the left, however it did not subsequently transmit the shock further. In addition, at some point later, at $t + T$, i.e. much later than the previous episode, the orange node acted as a source of a new shock that was transmitted to the subsequent blue node. Therefore, the orange node should be characterised either as an end-receiver in the first episode and as a source in the second episode. Such mis-characterisations can lead to misguided policies, founded on misinterpreted sources of financial contagion, as exemplified in case 2.

To address these limitations, we present a methodology that explicitly considers the time series of network topologies, aiming to uncover the dynamics of risk transmission and the contagion paths operating during crisis episodes. Our approach identifies the sequence of contagion events, distinguishing each country-sector pair, i.e. each node of the network, as either a source, a transmitter or receiver, and incorporates this information into node centrality metrics. For this purpose we utilise for the first time in the financial contagion literature some recently introduced mathematical tools for the study of dynamic networks, i.e. networks with time-varying topology (e.g. Scholtes et al. (2016)). Specifically, we employ higher-order aggregated network representations which are based on the underlying notion of time-respecting paths within a dynamic network topology. Generalised centrality metrics are computed in these higher-order

(a) Case 1: Contagion analysis using network snapshots: mis-characterisation of a transmitter node.

(b) Case 2: Contagion analysis using the aggregate network: missing the source of a financial shock.

Figure 1: Limitations of current network analysis approaches.

aggregated networks, encompassing information about time-varying topologies and reconstructing how financial contagion unfolds across sectors, countries and time. Therefore, our analysis moves beyond memoryless centrality metrics, derived either from static snapshots or averages across snapshots, and accommodates non-Markovian network features (Rosvall et al. (2014)), in which financial stress flows may depend on where stress originates from.

Our paper is related to a number of existing literature strands. The first of these strands investigates spillovers and shock amplification across segments of the financial system. For example, Gertler et al. (2016) present a canonical model with a retail and a shadow banking sector, modelled as wholesale funded entities, and show that shocks may spill from retail banks to shadow banks. In the stylised model of Meeks et al. (2017) banks and shadow banks are linked via securitised exposures and their balance sheets are again mutually affected by macroeconomic shocks. Allen and Carletti (2006) show how credit derivatives and other forms of credit transfer can lead to both contagion during crises and beneficial diversification. Empirical studies have utilised network metrics to investigate spillovers, e.g. Billio et al. (2012) find that causality links of the residual returns from banks, insurers and shadow banks started to increase just before and during the financial crisis (2006-2008). Specifically, the authors find that hedge funds unilaterally affected the banks, with no contagion transmission occurring in the opposite direction. In general, the authors conclude that banks and insurers represent sources or contagion more than shadow banks. However, this result does not hold when they employ a nonlinear Granger causality test. Chen et al. (2014) provide evidence that contagion mainly takes place from banks to insurers for a sample of US banks and insurers spanning the period

2002-2008. Wang et al. (2017) also identify banks as the main transmitters of systemic risk for a set of 84 S&P institutions during the period 2006-2015.

Another related strand of a growing empirical literature investigates spillovers across countries, mainly in the context of the European sovereign debt crisis. De Santis and Zimic (2017) find that connectedness across bond markets was on a downward path until 2012 when this path reversed, pointing to the fragmentation of the sovereign bond market. Blasques et al. (2016) examine the sovereign CDS of eight euro area countries and find that contagion within the euro area subsided after 2013. This is interpreted as the result of the policy measures undertaken during that period, namely the TLTRO and OMT programs of the ECB and the setting-up of the ESM. Spillovers across countries are examined also by Clayes and Vasicek (2014), Lee and Yang (2014), Fernandez-Rodriguez et al. (2016), Schwaab et al. (2017).

On the methodological level, our paper contributes to the growing empirical literature that studies financial contagion by adopting a network perspective. Studies that investigate networks based on direct exposures, either stocks or flows, proceed by either calculating centrality metrics or employing econometric methods to analyse the propagation of contagion (see e.g. Chinazzi et al. (2013), Langfield et al. (2014), Tonzer (2015), Brownlees et al. (2021), among others). Other studies employ Granger causality tests in means to construct causality networks among stock indices (Lee and Yang (2014), Billio et al. (2016)), sovereign bond yields (Caporin et al. (2018)) or multi-partite networks, e.g. combining stocks and sovereign bond yields (Corsi et al. (2018)). Brunetti et al. (2019) compare causality and physical networks formed in the interbank market of euro-area banks.

The centrality metrics used in the above studies are employed to identify the most interconnected nodes, i.e. which can be considered the most important for risk transmission. However, due to the methodology used, it is usually not possible to use these metrics to reliably distinguish between sources, transmitters or receivers of financial stress. This limitation could be especially important for studies that employ flow data of direct exposures or construct causality networks, due to the relatively high volatility of the network topology and the importance of the temporal dimension for a correct economic interpretation.[2]

In this paper we construct a time series of tri-partite Granger causality-in-tail networks

[2]The currently employed static methods seem well suited to analyse networks with slowly changing links, e.g. when links represent stock amounts that may vary slowly over time, or network topologies that incorporate all adjustments to external shocks due to transmission mechanisms operating almost instantly, e.g. when links represent price changes in highly liquid markets. In these cases the emphasis is on the structural properties of the network and not on the topology dynamics, e.g. as in Chinazzi et al. (2013).

and use Expected Default Frequency (EDF) data from Moody's Analytics. This approach enables a comprehensive analysis of the financial contagion channels that operated during the global financial crisis and its aftermath. In contrast, existing studies usually either investigate contagion across individual institutions within one national financial system or focus on cross-border contagion towards one specific country. Our study aims at enriching the literature that looks into the cross-country, cross-sectoral contagion simultaneously for a relatively larger set of countries, and is the first that looks into paths of causality-in-risk, simultaneously in both the country and financial sector dimensions.

We define contagion as incremental predictive power of a tail event conditional on the occurrence of tail events for the predictor variable in the right-hand tail of the distribution. Therefore, our study distinguishes contagion from interdependence by focusing on the predictive power in the tail. In addition, we use a GARCH filter addressing the critique that heteroscedasticity may bias tests for contagion (Forbes and Rigobon (2002)). We use a robust form of the Granger causality-in-distribution test proposed by Candelon and Tokpavi (2016), in which the test is run for different parameter values and kernel forms, thus addressing model uncertainty. The weight assigned to each edge connecting a pair of nodes is proportional to the number of parameter combinations that find this causality link, reflecting different degrees of certainty for contagion along this edge.

We find that the most typical sequence of contagion starts from either banks or shadow banks and much less frequently from insurance firms. The only exception to this pattern is observed during the global financial crisis of 2007-2010, when insurers were also sources of risk, consistently with default events that unfolded during that period and involved insurance firms. Furthermore, we find evidence that banks play the most important role as transmitters of financial stress within the financial network as they occupy much more frequently the intermediate nodes of time-respecting paths compared to other financial entities.

Our results also show that the temporal framework of analysis allows a clearer identification of the country shock origin compared to static approaches, consistently with the intuition behind the simple examples provided above. The static approaches that have been used so far to characterise nodes within financial networks tend to exalt the importance of large countries, such as the US or Japan, as sources of contagion while our approach is able to identify distress countries, such as Greece, Spain or Italy, as sources of shocks. This is explained by the focus of static approaches on synchronous and transmission paths of length one, leading to a bias

towards large countries.

Our work shares with Billio et al. (2017) and Billio et al. (2021a) a similar focus on the temporal dimension of networks applied to the analysis of risk transmission among countries and sectors (financial and real sectors). In these papers, an econometric framework is adopted based on multi-dimensional generalised matrices (tensors) that encapsulate information about time-varying network topologies. In our approach, the higher-order representation allows preserving the temporal dependence parsimoniously, simply based on the underlying edge evolution. The multilayer structure used in these studies is accommodated in our setting without imposing any layer structure a-priori. Our approach can also be seen as a dimensionality reduction technique, as by moving to an higher-order we reduce the number of nodes and links while preserving the temporal information.

The paper is structured as follows. Section 2 presents the methodology adopted for the construction of temporal networks based on Granger causality-in-risk. The higher-order network aggregation and the related centrality concepts are also introduced in this section. Section 3 presents the EDF dataset. Section 4 presents the results and Section 5 concludes.

2 Methodology

We present a methodology to empirically study contagion within a set of economic units (nodes) and across time, utilising time-varying network topologies. The economic units could be countries, regions, sectors or institutions. In this paper nodes represent country-financial sector pairs (e.g. 'Austrian banks' or 'Belgian insurance firms'), as elaborated in Section 3.

For this purpose, we construct a directed temporal network of risk transmission, i.e. a network with a time-varying topology where the directed edges represent incremental predictive ability of tail risk realisation on the receiver node, when the source node is included in the information set. Tail risk is realised when the default probability exceeds a specific VaR level. The temporal network is formally defined as a tuple $G^T = (V, E^T)$ comprising a set of nodes V and a set $E^T \subseteq V \times V \times [0, T]$ of time-stamped links $(x, y; t)$ corresponding to the presence of a link from node x towards node y during the time interval $[t, t + \Delta t]$. Δt is a unit of time during which the topology remains constant. The temporal network is observed during the period $[0, T]$ which comprises k intervals $[0, \Delta t], [\Delta t, 2\Delta t], ..., [(k-1)\Delta t, k\Delta t = T]$ each featuring (in general) a different topology. The set of nodes together with the fixed topology prevailing during a time

interval $[t, t+\Delta t]$ is denoted by G_t.

The links of the network represent contagion in the Granger sense and based on the ability of tail risk realisation in the transmitter node to enhance the prediction of tail risk realisation in the receiver node, as explained in more detail in the following Subection 2.1. Therefore, the links reflect potentially diverse transmission channels, either due to direct linkages, such as bilateral exposures, trade linkages, exposures to common risks, or to indirect mechanisms, e.g. related to increased risk aversion (Gai et al. (2011); Danielsson and Zigrand (2013)).[3]

2.1 A robust Granger causality-in-risk test

We introduce a robust version of the non-parametric test for Granger causality-in-distribution presented by Candelon and Tokpavi (2016) to identify statistical causality between two time series during tail events. The links of a temporal network are inferred by running the causality-in-distribution test consecutively for rolling time windows and for each country-sector pair. The test represents a multivariate extension of the test derived by Hong et al. (2009). Candelon and Tokpavi (2016) formulate the null hypothesis of no Granger causality-in-distribution between two stochastic processes, say Y_t and X_t, with direction $Y_t \rightarrow X_t$, by decomposing the distribution support of each series into a multivariate process of inter-quartile indicator variables derived from a VaR model that features a finite set of population parameters θ_X^0. In this way, causality-in-tail inference simultaneously considers different levels of the quantile, therefore avoiding inferences that are sensitive to the definition of a specific quantile.

In particular, let $m+1$ be the number of VaR percentiles $\alpha_s = \mathbb{P}\Big[X_t < VaR_{t,s}^X(\theta_X^0, \alpha_s)|\Omega_{t-1}^X\Big]$, with $s = 1, \ldots, m+1$, covering the whole distribution support $0\% \leq \alpha_1 < \cdots < \alpha_{m+1} \leq 100\%$. Then, $H_t^X(\theta_X^0) = (Z_{t,1}^X(\theta_X^0), \ldots, Z_{t,m}^X(\theta_X^0))'$ is an m-dimensional vector, indicating the percentile where the value of X_t lies for each t. Note that we do not need to consider all the sub-regions of the distribution, since m values suffice to identify the remaining region.[4] Moreover, by convention, $VaR_{t,s}^X(\theta_X^0, \alpha_s) = -\infty$ for $\alpha_s = 0\%$ and $VaR_{t,s}^X(\theta_X^0, \alpha_s) = \infty$ for $\alpha_s = 100\%$. The indicator function $Z_{t,s}^X(\theta_X^0)$ is activated whenever an event within the percentage range $\big[\alpha_s, \alpha_{s+1}\big)$ takes place

[3] Our focus is on Granger causality with respect to the occurence of tail events rather than identifying structural relationships among the nodes of the network. The identification of actual causal relationships in a multivariate setting is challenging as indirect and spurious causality may affect the conclusions. The literature starting with Hsiao (1982) investigates types of spurious causality and how techniques such as network analysis can be used to reconstruct causal chains (see also Eichler (2007)).

[4] Thereafter in this section we do not refer to the $m+1$ region.

$$Z^X_{t,s}(\theta^0_X) = \begin{cases} 1 & \text{if } X_t \geq VaR^X_{t,s}(\theta^0_X, \alpha_s) \ \& \ X_t < VaR^X_{t,s+1}(\theta^0_X, \alpha_{s+1}) \\ 0 & \text{else,} \end{cases} \tag{1}$$

for each $s = 1, \ldots, m$.

The null hypothesis of no Granger causality-in-distribution can then be written as

$$\mathbb{H}_0 : \mathbb{E}(H^X_t(\theta^0_X)|\Omega^{X\&Y}_{t-1}) = \mathbb{E}(H^X_t(\theta^0_X)|\Omega^X_{t-1}) \tag{2}$$

where $\mathbb{E}()$ is the expectation operator, Ω_{t-1} is a filtration[5] up to $t-1$, which may contain information either on both X_t and Y_t or only on X_t.

We further denote by $\hat{\Gamma}_X$ and $\hat{\Gamma}_Y$ the sample correlation matrices of the estimated $\hat{H}^X_t$ and $\hat{H}^Y_t$, respectively. In addition, we also define the sample cross-covariance and cross-correlation matrices between $\hat{H}^X_t$ and $\hat{H}^Y_t$. The sample cross-covariance matrix equals $\hat{\Lambda}(j) = T^{-1}\sum_{1+j}^{T}(\hat{H}^X_t - \hat{\Pi}_X)(\hat{H}^Y_{t-j} - \hat{\Pi}_Y)$ for $0 \leq j \leq T-1$ and $\hat{\Lambda}(j) = T^{-1}\sum_{1-j}^{T}(\hat{H}^X_{t+j} - \hat{\Pi}_X)(\hat{H}^Y_t - \hat{\Pi}_Y)$ for $1-T \leq j \leq 0$, where $\hat{\Pi}_X$ (respectively $\hat{\Pi}_Y$) is the sample mean of $\hat{H}^X_t$ (respectively $\hat{H}^Y_t$). Consequently, the sample cross-correlation matrix $\hat{R}(j)$ is equal to $\hat{R}(j) = D(\hat{\Sigma}_X^{-1/2})\hat{\Lambda}(j)D(\hat{\Sigma}_Y^{-1/2})$, with $\hat{\Sigma}_X$ and $\hat{\Sigma}_Y$ representing the sample covariance matrices of the estimated event variables $\hat{H}^X_t$ and $\hat{H}^Y_t$ and $D()$ is the diagonalization operator.

The test utilises the following quadratic expression of cross-correlations between the indicator vectors for X_t and Y_t

$$\hat{Q}(j) = Tvec(\hat{R}(j))'(\hat{\Gamma}_X^{-1} \otimes \hat{\Gamma}_Y^{-1})vec(\hat{R}(j)) \tag{3}$$

with $vec()$ denoting the vectorization operator and $\otimes$ the Kronecker product.

Specifically, the test is based on the following kernel-weighted sum of past $\hat{Q}(j)$s

$$\hat{\mathcal{T}} = \sum_{j=1}^{T-1} \kappa^2(j/M)\hat{Q}(j) \tag{4}$$

where $\kappa()$ represents a kernel that discounts past values[6] and M is a truncation parameter

[5] A filtration is an increasing sequence of σ-algebras. In turn, a σ-algebra on a certain set is a collection of subsets (including the whole set itself) that is closed under complement and countable unions. Filtrations represent essentially information up to a certain time and are useful to define conditional expectations.

[6] We follow Hong et al. (2009) and Candelon and Tokpavi (2016) and define the kernel to be a symmetric function on the real line with co-domain $[-1, 1]$ and continuous at zero with at most a finite number of discontinuity points, so that: (i) $\kappa(0) = 1$; (ii) $\int_{-\infty}^{\infty} \kappa^2(z)dz < \infty$.

dependent on the sample size T so that $M \to \infty$ and $M/T \to 0$ as $T \to \infty$.[7]

Using the above notation, the following test statistic is used to test the hypothesis in (2) (after scaling and centering $\hat{\mathcal{T}}$):

$$V_{Y \to X} = \frac{\hat{\mathcal{T}} - m^2 C_T(M)}{(m^2 D_T(M))^{1/2}} \tag{5}$$

where $C_T(M) = \sum_{j=1}^{T-1}(1 - j/T)\kappa^2(j/M)$, $D_T(M) = 2\sum_{j=1}^{T-1}(1 - j/T)(1 - (j+1)/T)\kappa^4(j/M)$.

Following Candelon and Tokpavi (2016), our default parameterisation of the test involves the use of the Daniell kernel $\kappa(x) = sin(\pi x)/\pi x$ and choosing $M = [1.5T^{0.3}]$. To ensure that our results are not sensitive to these choices we also implement a robust form of the test whereby the test results for three different kernels and three different truncation parameters are aggregated. In this robust form of the test we employ all combinations of different kernel functions (uniform, Bartlett and Daniell kernels) and different values for the truncation parameter M ($M = [1.5T^{0.3}]$, $M = [ln(T)]$ and $M = [2T^{0.3}]$), calculate the weighted sum, where the weights reward evidence of Granger causality. This is a model averaging approach that reduces uncertainty over the results which could be induced by the choice of the kernel function and the truncation parameter.

The quadratic form in (4) is based on the squared absolute distance between kernel estimators of the cross-spectral density without and with the restriction imposed by the null hypothesis. When this distance is sufficiently large, the null hypothesis of no Granger causality-in-distribution is not confirmed. However, in a financial contagion context we are not interested in the whole distribution as interdependence relationships in normal times may not correspond to active links transmitting contagion during financial stress. We thus focus on financial stress events by selecting the appropriate VaR levels, and we consider the right tail of the EDF distribution, representing high default risk, in order to form a network whose links represent added predictive ability of tail risk.[8] Therefore, we investigate causality-in-distribution using the VaR levels $A = \{90\%, 95\%, 99\%, 100\%\}$, i.e. $m + 1 = 4$. Technical details about the VaR model have been relegated to Appendix A.

[7] The M parameter reflects the degree to which lagged values are considered.

[8] This is in contrast to other studies that utilise e.g. stock returns where the left tail is the one corresponding to extreme negative shocks.

2.2 A tail risk statistical causality network

Using the robust version of the above-described test, we construct a network whereby nodes represent country-sector pairs and edges change over time. Our focus is to identify country-sector pairs which are critical in risk transmission and investigate the relative importance of the various financial sector segments and countries.

The calculation of node centrality metrics, e.g. node degree, closeness, betweenness and eigenvector centrality, is the standard approach to identify critical nodes and investigate the topological properties of a network. Existing applications of network theory in finance and economics employ these concepts of centrality, applied each time to a given network topology (for example, see Bonaccolto et al. (2019), Billio et al. (2012), Chinazzi et al. (2013) and Corsi et al. (2018)). Specifically, assuming a temporal network with topological dynamics $G^T = (V, E^T)$ for the observation period $[0, T]$, comprising a set of nodes V and a set of time-stamped links $E^T \subseteq V \times V \times [0, T]$, node metrics are computed for each topology separately, i.e. for each G_t, where the unit of time Δt represents the minimum time for which the network topology can be considered as constant. Therefore, a centrality metric $C(\cdot)$ for each node v is specific to the current topology, i.e. $C_t(v) = f(G_t)$.

This standard approach provides insights into how the structural features of the network are changing throughout time, however it is memoryless as it focuses only on the links existing synchronously. Therefore, it does not consider transmission mechanisms operating with a delay longer than Δt. Another approach, which is also used in the financial contagion literature, is to aggregate the time-stamped links into a single network where the weights in the time-aggregated network are related to the number of times that a specific link is found. Specifically, we can define the (first-order) time-aggregated network $G^{(1)} = (V, E^{(1)})$ based on the aggregated temporal links $E^{(1)} \subseteq V \times V$. This means that two nodes $v_1, v_2 \in V$ will be connected in $G^{(1)}$ whenever there is at least one $t \in [0, T]$ for which $(v_1, v_2; t) \in E^T$.[9] In that case, the corresponding centrality measure $C^{(1)}(v)$ is a function of the temporal network $f(G^T)$; however, the sequence with which the topologies G_t occurred does not impact the value of the centrality metric and therefore potentially critical information is not utilised. Specifically, if we consider an alternative temporal network $\acute{G}^T$ which is identical to G^T except from two points in time t_1 and t_2 for which the corresponding time-stamped network instances are reversed, i.e. $\acute{G}_{t_1} = G_{t_2}$ and $\acute{G}_{t_2} = G_{t_1}$,

[9] Depending on the application, the weights of the network can be defined to reflect the total duration for which the link between v_1 and v_2 has persisted.

the centrality measures calculated for $\acute{G^T}$ would be the same as for G^T since the respective aggregated networks are identical, i.e. $\acute{G^{(1)}} = G^{(1)}$. Therefore, potentially critical information on the temporal sequence is lost and the economic interpretation may be distorted.

To summarise, when considering individual topologies or the time-aggregated network, the information content of the dynamics and, specifically, how paths are created across the changing topologies is not utilised.[10] However, the phenomenon of contagion entails the transmission of stress from one agent to another and then *at a subsequent point in time* to a third. Such dynamic paths spanning different periods are essential when analysing the transmission of contagion and to identify origins, transmitters and receivers of financial stress.

In addition, network analyses from the perspective of either static or time-aggregated networks assume the transitivity property which is fundamental for the definition of the standard centrality metrics: namely that the existence of links $a \to b$ and $b \to c$ implies that a path $a \to b \to c$ of stress transmission is operating. One can easily imagine situations in which whether the existence of such a path can be inferred depends on the timing of the past links that lead to node c, e.g. if the two links $a \to b$ and $b \to c$ occurred in the opposite order or $a \to b$ occurred much earlier than $b \to c$, then the inference of a path $a \to b \to c$ is not plausible. Time-aggregated networks, for example, do not consider the sequencing of edges and therefore may assume transitivity also in cases where this property does not apply, potentially leading to a distortion in the set of identified paths. This distortion could overestimate the centrality of nodes which exhibit relatively many links across the various topologies (e.g. large countries), as the transitivity assumption would make them appear as parts of many long paths (and consequently attain high values of centrality) even if these paths do not actually respect the transitivity property.

The example in Figure 2 illustrates the importance of considering the dynamics of the network topology. The figure shows three cases where the same topology has different interpretations depending on the timing of each edge. In the static network case (case (a)), we consider only the links existing at a specific point in time (or equivalently the total number links throughout a period, as in a time-aggregated network). One could infer from this topology that node b acts as an amplifier node, by transmitting financial stress from the source node a towards nodes c and d.

When one considers the timing of links, the conclusion may differ sharply. In the second

[10] To make an analogy with econometrics, it is akin to analysing a panel dataset either as separate cross-sections or as a pooled dataset neglecting the correlations of observations across time.

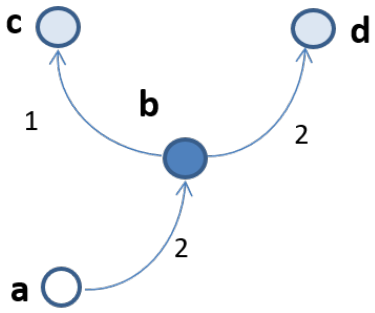

(a) Static network or time-aggregated network

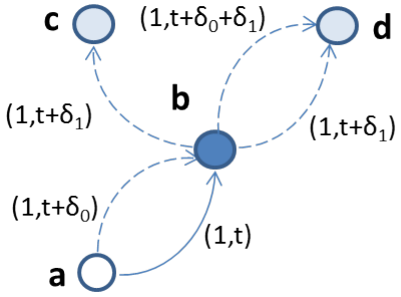

(b) Time-varying network with time-respecting paths

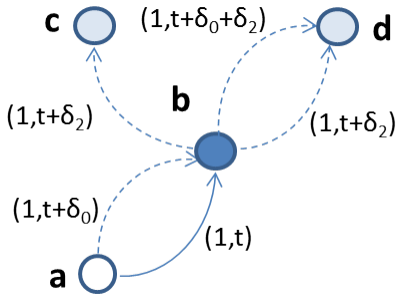

(c) Time-varying network without time-respecting paths

Figure 2: Topological properties are sensitive to the network dynamics. It is assumed that $\delta_1 < \delta \ll \delta_2$ where δ represents the maximum time required for financial stress to be transmitted from a node to another. The numbers in (a) represent the weights of each link. For each link in (b) and (c) the corresponding parenthesis contains the weight and the timing, respectively.

case, (b), node b receives two inward links (i.e. representing financial stress from a at time t and $t + \delta_0$, respectively), which are followed by outward links (i.e. further transmission of financial stress) occurring within a delay δ_1 that is comparable to the scale Δt of the financial contagion phenomenon. Therefore, the conclusion remains similar to that of case (a). However, in the third case, (c), the outward links occur within a lag $\delta_2 \gg \Delta t$. Consequently, it would be misleading to attribute the links from b towards c and d to a further transmission of stress which node b received from node a. It would be more plausible to infer that two independent contagion phenomena have taken place, the first being a contagion from source node a towards receiving node b and the second with node b as the source and nodes c and d at the receiving end. Therefore, node b functions here as a source while the analysis of the time-aggregated network would lead to a misleading conclusion that it is a transmission node.

The scale of the phenomenon under discussion, as measured by the value of Δt, is therefore a critical parameter to distinguish paths across time and the proper identification of the role

played by the various nodes during contagion. In other words, the ordering of the edges needs to be complemented by their timing in order to define a path comprising edges that occur at different points in time. In this context, we would need to define generalised centrality metrics that would incorporate information about time-varying topologies such as those depicted in Figure 2 to properly account for contagion dynamics and systemic relevance of the network nodes. Such metrics should distinguish between related and unrelated paths and should be informed by a relevant time horizon parameter Δt.

The concept of time-respecting paths (Scholtes et al. (2016)) enables reconstructing chains of contagion episodes across multiple nodes over time. A time-respecting path is a collection of triples composed of a sender node, a receiver node and a time snapshot when the link between sender and receiver occurred, for all times recorded. Formally, a time-respecting path between nodes v_0 and v_l with a maximum time difference δ is defined as a sequence $(v_0, v_1; t_1), ..., (v_{l-1}, v_l; t_l)$ in which the time-stamps of the links in the path is increasing, i.e. $t_1 < t_2 ... < t_l$ and, in addition, $0 < t_{i+1} - t_i < \delta$, for $i = 1, ..., l-1$.

In our context, time-respecting paths represent contagion chains tracing the paths of transmission for arbitrary lengths, i.e. determining sequences of Granger causality-in-tail of length greater than one (i.e. not only just a link, but time-respecting chains of links). For instance, we are interested in investigating whether the global financial crisis originated e.g. mainly from shadow banks to then affect banks and insurers and finally feed back to shadow banks. Using the notion of time-respecting paths we can understand the role of financial market segments in the contagion episodes, i.e. whether they act as sources, transmitters or receivers.

An additional appealing feature of the temporal network analysis, as regards its use to study economic phenomena and specifically financial contagion, is the ability to distinguish transmission channels operating across various time scales. Standard centrality measures calculated in individual topologies are based on synchronous paths, i.e. network paths that exist in a specific topology, which are assumed to reflect the economic links existing for a short period, e.g. $[t, \Delta t]$. On the other hand, time-respecting paths and the generalised centrality measures consider also paths formed across longer time lengths, reflecting more slowly-moving transmission channels. For example, such channels may include those caused by changes in volumes, such as credit crunches, investment adjustments, or sticky price adjustments.

The analysis of temporal networks based on the time-aggregated network representation is underpinned by implicit Markovian assumptions. Specifically, it is assumed that the existence

of an edge does not depend on previous edges preceding it. In contrast, the approach adopted in this paper is able to accommodate non-Markovian temporal network features. The reference to (non-)Markovian features of a network can be further made clearer by considering the mapping which exists between a temporal network and a transition matrix comprising the probability of a random walker jumping to another node from each node in the network (Scholtes et al. (2014)). When a time-aggregated network is examined, the construction of the corresponding transition matrix considers each specific edge individually, without any reference to potentially related edges and their timing. An expanding recent literature has moved beyond this (essentially static) approach and investigated non-Markovian network features (Rosvall et al. (2014); Scholtes et al. (2014); Scholtes et al. (2016)). However, to our knowledge, this strand of temporal network analysis has not found application in economics and finance.

In this work we follow this literature on modelling non-Markovian characteristics of temporal networks and compute centrality measures taking into account the network dynamics. For this reason we employ the notion of higher-order aggregate network (Scholtes et al. (2014)) which is a Markovian representation of non-Markovian temporal networks. Specifically, a nth-order aggregate network $G^{(n)}$ comprises nth-order nodes $V^{(n)} \subseteq V^n$ and nth-order edges $E^{(n)} \subseteq V^{(n)} \times V^{(n)}$ whereby each existing edge represents a time-respecting path in the original temporal network and the weight of the edge reflects the frequency with which the time-respecting path occurs. Formally, a nth-order edge (υ, ω), where $\upsilon = (\upsilon_1, \ldots, \upsilon_n)$ and $\omega = (\omega_1, \ldots, \omega_n)$ are n-tuples, exists if and only if υ and ω overlap in $n-1$ elements as follows

$$(\upsilon_1, \upsilon_2 = \omega_1; t_1), ..., (\upsilon_n = \omega_{n-1}, \omega_n; t_n) \tag{6}$$

thus defining a path of length n in the original network. The edge will exist in the nth-order aggregated network if and only if in the temporal network a set of $\{t_1, ..., t_n\}$ exists for which the above path is a time-respecting path for a given δ. The weight of the edge is given by

$$w(\upsilon, \omega) = |\{(\upsilon_1, \upsilon_2 = \omega_1; t_1), ..., (\upsilon_n = \omega_{n-1}, \omega_n; t_n) : 0 < t_{i+1} - t_i < \delta\}|. \tag{7}$$

A nth-order aggregated network accomodates non-Markovian features, as the nth edge $(\upsilon_n = \omega_{n-1}; \omega_n)$ of a time-respecting path of length n depends on the $n-1$ previous edges.

Generalised centrality metrics can be computed on the nth-order aggregate network to obtain economically meaningful rankings of systemic importance. Scholtes et al. (2016) show

that second-order centralities better approximate temporal centralities compared to static centralities, which are normally used in the economics and finance literature. The second-order betweenness centrality can be defined as

$$BC^{(2)}(v) = \sum_{\substack{x \neq y \in V, \\ u-x \in V^{(2)}, \\ y-w \in V^{(2)}}} |\{p \in P^{(2)}(u-x, y-w; v) : len(p) = dist^{(2)}(u, w)\}| \tag{8}$$

where $P^{(2)}(u-x, y-w; v)$ is the set of shortest time-respecting paths across all starting times connecting vertex $u-x$ to $y-w$ in the second-order network via v in the first-order network, $dist^{(2)}(u, w) = min_{r,z \in V^{(2)}, r=u-*, z=*-w} L^{(2)}(r, z) + 1$ is a second-order distance function and $L^{(2)}(r, z)$ denotes the length of a shortest path between two arbitrary second-order nodes $r, z \in V^{(2)}$, where, in turn, $V^{(2)}$ is the set of (second-order) nodes.[11]

The second order out-closeness centrality is defined as

$$CC^{(2)}(v) = \sum_{u \neq v} \frac{1}{dist^{(2)}(u, v)} \tag{9}$$

where for each node in the network, we sum the inverse distances *towards* all other nodes according to the topology of the second-order aggregate network. Alternatively, the second order in-closeness centrality considers distances *from* all other nodes of the network.

Finally, we also compute the standard first order centralities for each network instance (i.e. the topology corresponding to an interval $[t, t + \Delta t]$) and examine their evolution over time. The first order betweenness centrality is given by

$$BC_t^{(1)}(v) = \sum_{u \neq v \neq w} P_t^{(1)}(u, w; v) \tag{10}$$

where $P_t^{(1)}(u, w; v)$ is the set of those shortest paths from node u to w in a static network that pass through node v. The first-order out-closeness centrality is given by

$$CC_t^{(1)}(v) = \sum_{u \neq v} \frac{1}{dist_t^{(1)}(u, v)} \tag{11}$$

where $dist_t^{(1)}(u, v)$ is the first-order distance, that is the length of a shortest path, from node u to v in the first-order aggregate network. The subscript t denotes the time snapshot when the cen-

[11] The notation $a - b$ stands for a second-order node.

trality is computed. The first order in-closeness centrality is defined using instead $dist_t^{(1)}(v,u)$.

The joint evaluation of the first order centralities calculated for each snapshot topology complements the second order analysis which looks holistically into the whole sequence of topologies.

3 Data

We utilise EDF data provided by Moody's Analytics. The EDF represents a risk measure derived by combining balance sheet information and market fundamentals. Compared to stock or CDS prices, EDF are less affected by frictions, which are especially prevalent during crisis periods, such as liquidity risk, strategic trading and counterparty risk (Jarrow (2012) and Tang and Yan (2010)). Similarly, Bongaerts et al. (2011) argue that CDS prices, which are often used in the related literature, should not be considered as a pure measure of credit risk due to the impact of liquidity on them. Therefore, the use of EDFs allows a clearer focus on the credit risk characterising the underlying entities. In addition, compared to equity returns, EDFs quantify the firm's default probability, which is a more relevant factor when considering the propagation of contagion compared to the shareholders' expected return.

The data on EDFs are locational in nature, span the period from 1 January 2006 to 7 February 2018 (in total 3050 days), and cover a set of 16 advanced economies. These economies are Austria, Belgium, Finland, France, Germany, Greece, Ireland, Italy, Japan, the Netherlands, Portugal, Slovakia, Spain, Sweden, the UK, and the US.

EDFs represent daily estimates of forward-looking probabilities of default within a one year horizon (EDF 8 and EDF 9 models). Estimation is based on an option-pricing model utilising Vasicek's formulation of option contracts. Country- and industry-level volatility estimates and credit risk information are used to compute a distance-to-default measure which is mapped against the probability space.[12]

Our sample covers the three main components of the financial system, namely banks, shadow banks and insurers, thus enabling a study of contagion across aggregated country-sectors. Locational data are well-suited for that purpose, as foreign entities which may belong to a parent entity are not consolidated and risk transmission across entities from different countries that belong to the same financial conglomerate can be identified. The banking sector is represented by Moody's industry code N06 that includes banks and savings and loan associations. The

[12]More details are available at https://www.moodysanalytics.com/-/media/whitepaper/2015/2012-28-06-public-edf-methodology.pdf

insurance sector comprises codes N29 and N30, i.e. life insurance and property/casualty/health insurance, respectively. Shadow banks include codes N23 (Finance Companies), N24 (Finance - not elsewhere classified), Investment Management (N31), Real Estate Investment Trusts (N47), Security Brokers and Dealers (N48). Institutions can change industry over time. Our sample includes publicly traded firms, therefore includes entities that are in general more exposed to market signals.

Consistently with other studies (Candelon and Tokpavi (2016) and Podlich and Wedow (2014)), we retain all institutions in the sample, thus considering also those that disappeared at some point in time from the sample or companies that entered the sample after the beginning of the sample period. This is consistent with our aim to identify spillovers at the country level. If we studied only the sample that is present throughout the entire period the sample size would be significantly reduced, and survival bias would be introduced.

Similarly to Podlich and Wedow (2014), EDF changes are expressed as a weighted average for each country-sector pair and computed using: i) each company's asset value, which is estimated by Moody's to reflect the market's view of the value of a company in light of its equity value, equity volatility and liability structure; ii) the EDF1 of each company, which is Moody's calculated expected default frequency value within a year (EDF 9 model), expressed in percentages. In this framework, a default event occurs in case of failure of a principal or interest payment or a government bailout. EDFs are regarded as a measure of the default probability; and iii) total assets computed as the sum of the asset values of the institutions included in the sample of each jurisdiction.

In the analysis that follows we also consider separately four different periods corresponding to a commonly used periodisation of the last fifteen years as regards the different phases of the financial crisis. The first one, which we label as the 'pre-crisis' period is up until August 2007, when hedge funds Bear Stearns High-Grade Structured Credit Strategies Fund and Bear Stearns High-Grade Structured Credit Strategies Enhanced Leveraged Fund filed for bankruptcy. The second period corresponds to the global financial crisis and runs until the onset of the Greek crisis in April 2010. This event defines the start of the third period, the European financial crisis, which ends with Mario Draghi's London speech of July 2012 and marks the beginning of the fourth and last period, featuring a number of less intense crisis episodes, especially after 2015 (see Billio et al. (2016)).

Figure 3 plots the aggregate EDFs for each country and financial segment separately for two

sets of countries in the sample. These are 'large' countries (the US, Japan, the UK, Germany and France)[13] and 'distress' countries (Italy, Spain, Ireland, Greece, Portugal) that includes four countries that required at some point in time financial assistance programs in addition to Italy where episodes of political instability were followed by financial turbulence. Overall, the most elevated risk levels were observed during the global and the European financial crises, with bouts of financial stress occurring after Mario Draghi's speech in 2012 especially in the banking sectors of 'distress' countries after 2015. A significant degree of heterogeneity across countries and financial institutions is apparent. For example, the risk for insurance companies was highest until 2012 and since then it has remained at relatively low levels while banks and shadow banks have experienced relatively high risk levels also during the post-2012 period. Furthermore, the group of 'large' countries experienced elevated levels of risk mainly during the global financial crisis while the 'distress' countries were much more impacted later, after 2010.

The summary statistics of Table 1 show that overall shadow banks have higher credit risk compared to banks while insurances represent the least risky financial segment, a risk ranking which is consistent when either the mean, the median or the 3rd quartile of the distribution is considered.[14]

As expected, the Greek, Belgian, Portuguese, Irish, Spanish and Italian banking sectors stand out in terms of riskiness. Similar is the situation for the insurance sector, with the US insurance sector also exhibiting high risk. The shadow banking sector is more idiosyncratic and the US is on the top of risk, followed by Greece and Portugal, when the mean value is considered.

Table 1: Summary statistics of EDFs. EDFs are expressed as percentages. Source: Moody's Analytics and authors' calculations.

Sector-country	Mean	Min	1st quartile	Median	3rd quartile	Max
Banks	1.43	0.01	0.24	0.54	1.27	21.76
Austria	1.07	0.02	0.40	0.89	1.53	4.09
Belgium	4.84	0.03	0.32	0.65	12.62	16.54

[13]The first set includes the largest economies in the sample, which did not require financial assistance nor faced the risk of losing market access for their sovereign debt issuance.

[14]We conducted a preliminary statistical analysis, not reported here, using the tests on the equality of means and the Wilcoxon rank-sum (Mann-Whitney) test. It was found that the average EDF is statistically lower for the pre-crisis periods compared to all other phases (for all three financial sectors). EDFs attain their highest values for the banking and insurance sector during the European phase of the crisis while for the shadow banking sector the peak of risk is associated with the global financial crisis period.

Table 1 – continued from previous page

Sector-country	Mean	Min	1st quartile	Median	3rd quartile	Max
Germany	1.81	0.12	0.30	1.12	2.80	7.52
Spain	0.58	0.01	0.20	0.44	0.71	3.20
Finland	0.44	0.01	0.16	0.38	0.57	1.66
France	0.70	0.01	0.27	0.43	0.99	3.69
Greece	4.72	0.07	0.56	2.45	6.52	21.69
Hungary	0.90	0.07	0.46	0.63	0.90	10.27
Ireland	1.99	0.03	0.24	1.63	2.94	14.73
Italy	0.96	0.01	0.25	0.63	1.47	4.52
Japan	2.13	0.10	0.46	0.82	3.69	9.89
Luxemburg	0.11	0.10	0.10	0.11	0.12	0.16
Netherlands	0.74	0.01	0.29	0.47	0.77	3.77
Portugal	2.31	0.04	0.50	1.23	2.37	16.71
Slovakia	0.82	0.01	0.17	0.73	1.14	4.16
Sweden	0.26	0.03	0.11	0.26	0.38	1.36
United Kingdom	0.53	0.02	0.14	0.42	0.72	2.78
United States	0.67	0.03	0.10	0.30	1.20	4.21
Insurance firms	1.23	0.01	0.17	0.46	1.07	27.62
Austria	0.42	0.06	0.18	0.37	0.59	1.46
Belgium	2.09	0.01	0.01	0.06	0.17	19.76
Germany	0.46	0.05	0.20	0.31	0.74	1.45
Spain	0.36	0.01	0.12	0.33	0.52	1.91
Finland	0.09	0.01	0.04	0.06	0.14	0.27
France	0.51	0.03	0.28	0.40	0.70	2.32
Greece	6.16	0.07	0.86	2.94	9.33	27.62
Hungary	1.70	0.41	1.15	1.49	2.29	3.68
Ireland	3.26	0.04	0.79	2.42	5.05	16.30
Italy	0.97	0.06	0.32	0.48	0.95	5.01
Japan	1.34	0.16	0.50	0.78	2.29	4.99
Luxemburg	0.39	0.08	0.17	0.34	0.51	1.45

Table 1 – continued from previous page

Sector-country	Mean	Min	1st quartile	Median	3rd quartile	Max
Netherlands	1.03	0.02	0.41	0.75	1.15	5.40
Slovakia	1.44	1.12	1.33	1.46	1.57	1.61
Sweden	0.31	0.09	0.22	0.36	0.38	0.72
United Kingdom	0.59	0.05	0.26	0.58	0.82	1.57
United States	1.52	0.04	0.35	0.53	2.77	11.15
Shadow banks	3.10	0.00	0.21	0.73	2.58	35.02
Austria	3.00	0.01	0.27	0.66	1.85	28.17
Belgium	1.85	0.03	0.06	0.30	1.34	11.68
Germany	3.32	0.03	0.51	1.20	2.05	32.62
Spain	0.66	0.01	0.13	0.27	0.63	9.25
Finland	0.19	0.01	0.02	0.08	0.17	3.81
France	0.46	0.02	0.18	0.29	0.43	4.27
Greece	8.94	0.02	1.89	7.02	12.79	29.31
Hungary	3.59	0.17	1.11	2.04	4.97	17.71
Ireland	3.53	0.01	0.06	0.28	0.58	29.03
Italy	2.28	0.08	0.63	1.81	2.66	14.05
Japan	3.21	0.23	1.07	2.36	4.74	13.94
Luxemburg	0.87	0.01	0.05	0.60	1.51	4.21
Netherlands	0.54	0.05	0.24	0.44	0.65	2.83
Poland	1.57	0.05	0.79	1.49	2.36	4.59
Portugal	7.01	0.00	1.74	6.60	10.57	32.96
Slovakia	5.51	0.06	0.42	0.88	5.52	32.85
Sweden	0.44	0.06	0.17	0.37	0.65	7.22
United Kingdom	1.69	0.09	0.52	1.05	1.73	10.86
United States	9.75	0.21	8.17	11.94	12.91	17.00

(a) Banks - large countries

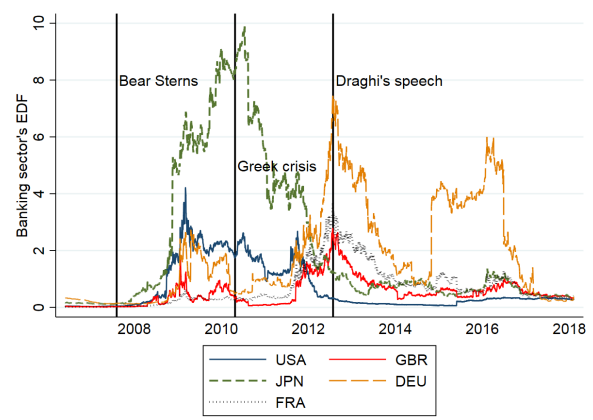

(b) Banks - distress countries

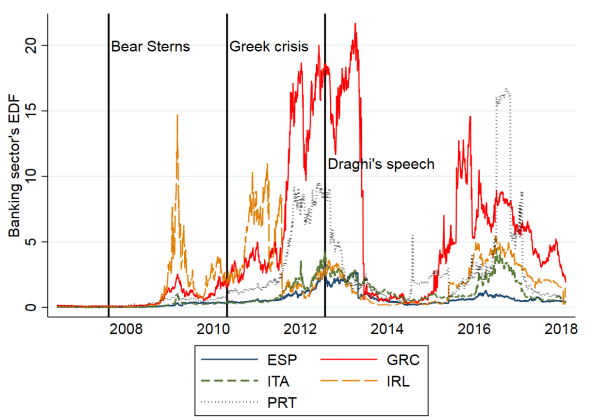

(c) Insurance - large countries

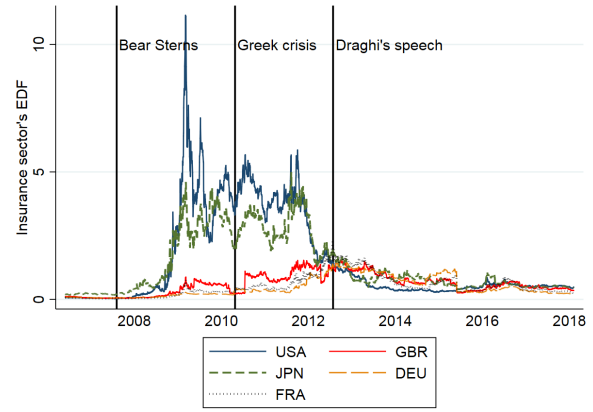

(d) Insurance - distress countries

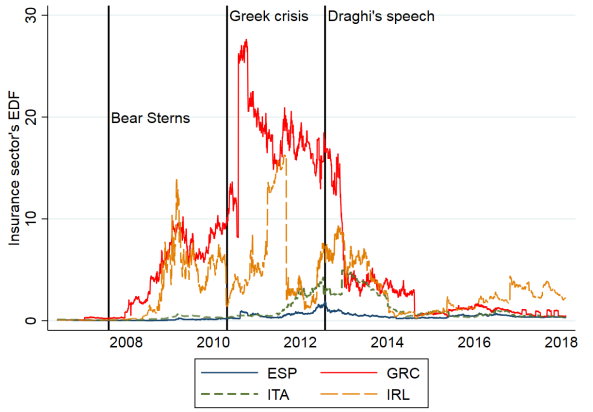

(e) Shadow banks - large countries

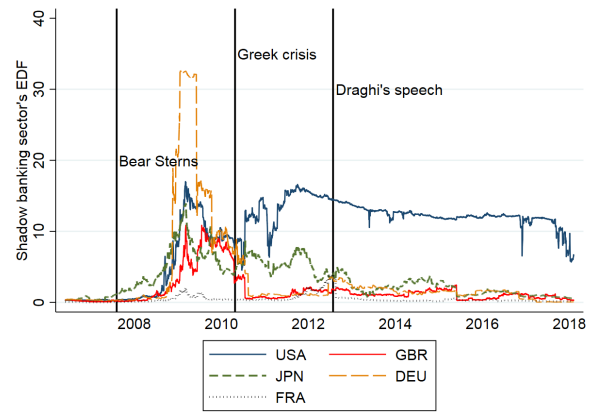

(f) Shadow banks - distress countries

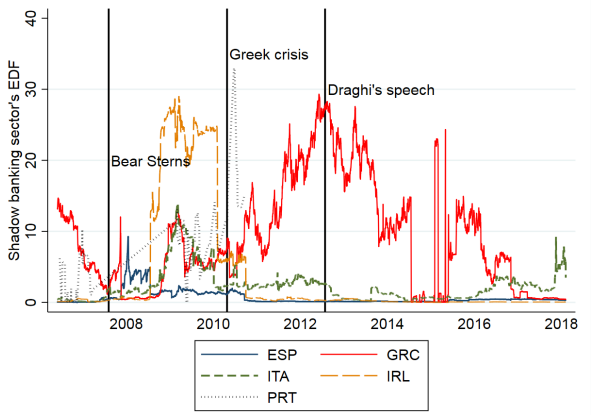

Figure 3: EDFs for different financial sector segments and countries. EDFs are expressed as percentages. Four periods of the sample period are marked by the three vertical lines. Source: Moody's Analytics and authors' calculations.

4 Empirical analysis

This section provides the empirical results. Subsection 4.1 presents the sequence of Granger causality-in-risk networks obtained and how the basic properties of this sequence reflect the

periods of financial distress. Subsection 4.2 employs standard measures of node centrality to gauge the relative importance of countries and sectors in the contagion transmission. Subsection 4.3 extends this analysis using the tools of higher-order aggregate networks to account for the dynamic topology of the network and compares the findings with those of the static network analysis. Subsection 4.4 investigates contagion patterns across sectors.

4.1 Network macro-features and validation

We estimate Granger causality-in-risk for each country-sector pair, i.e. in total $(16\times3)^2 - (16\times3) = 2,256$ times, where 16 is the number of countries and 3 is the number of financial sectors. The tests are run at each iteration for a rolling sample spanning $12\times30 = 360$ observations, which is increased by 30 observations for each new iteration. In this way, 90 network topologies are constructed.

The evolving topology of the network is shown in Figure 4, where 9 network snapshots are visualised, spanning in an equidistant way the whole range of network instances.[15] We observe that the density of the network fluctuates significantly across time periods and intensifies with the severity of the crisis. The increasing density during periods of elevated financial stress has been noted in the literature and renders our results consistent with those derived in Brunetti et al. (2019) for correlation networks.[16]

Figure 5 reports the density of the network against the Composite Indicator of Systemic Stress (CISS) published by the European Central Bank (see Holló et al. (2012)). All in all, the network density closely tracks the CISS. Financial stress during the global financial crisis and the European phase of the crisis is mirrored in the evolution of both the CISS and network density. The CISS places relatively more weight on situations where stress is simultaneously elevated in various market segments.[17] On the other hand, the network density increases when causality-in-risk is present for more country-sector pairs. The turbulence of 2015-2017, characterised by the Greek referendum, emerging markets volatility, a slump in the Chinese stock market and the UK referendum, is reflected more intensely in the network density compared to the CISS. However, all in all, the pattern seen in the network density and the CISS is very similar.

To further investigate the macro-properties of the network, we compute the time-aggregated

[15] To visualise the sequence of networks in a video please visit: https://youtu.be/_g__5JTVN68.

[16] This pattern is reversed for direct exposure networks, as interbank lending freezes or fragmentation takes place during periods of elevated risk.

[17] The CISS considers money, bond, equity and foreign exchange markets in addition to market indices linked to financial intermediaries.

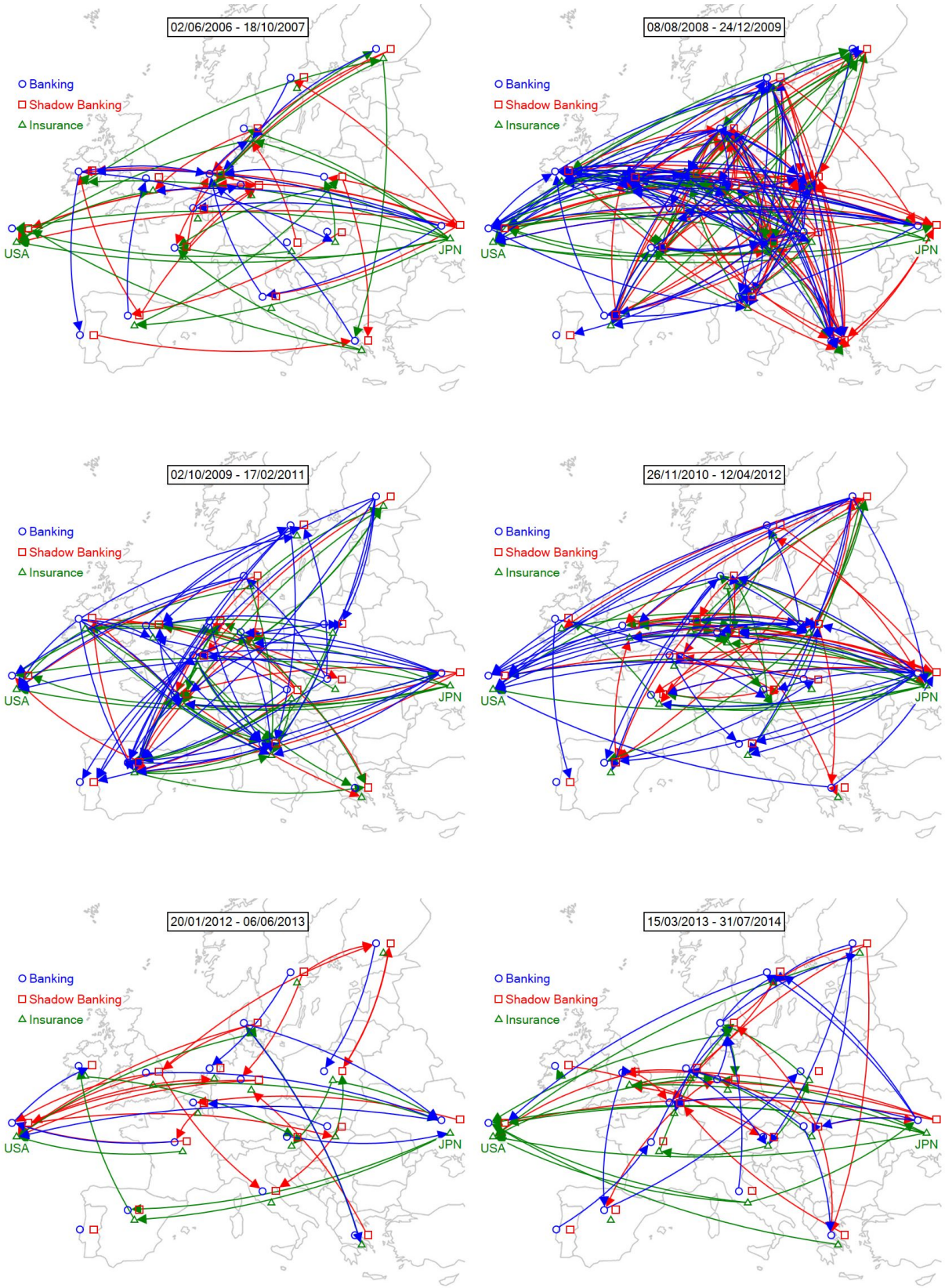
02/06/2006 - 18/10/2007
Banking
Shadow Banking
Insurance
USA
JPN
08/08/2008 - 24/12/2009
Banking
Shadow Banking
Insurance
USA
JPN
02/10/2009 - 17/02/2011
Banking
Shadow Banking
Insurance
USA
JPN
26/11/2010 - 12/04/2012
Banking
Shadow Banking
Insurance
USA
JPN
20/01/2012 - 06/06/2013
Banking
Shadow Banking
Insurance
USA
JPN
15/03/2013 - 31/07/2014
Banking
Shadow Banking
Insurance
USA
JPN

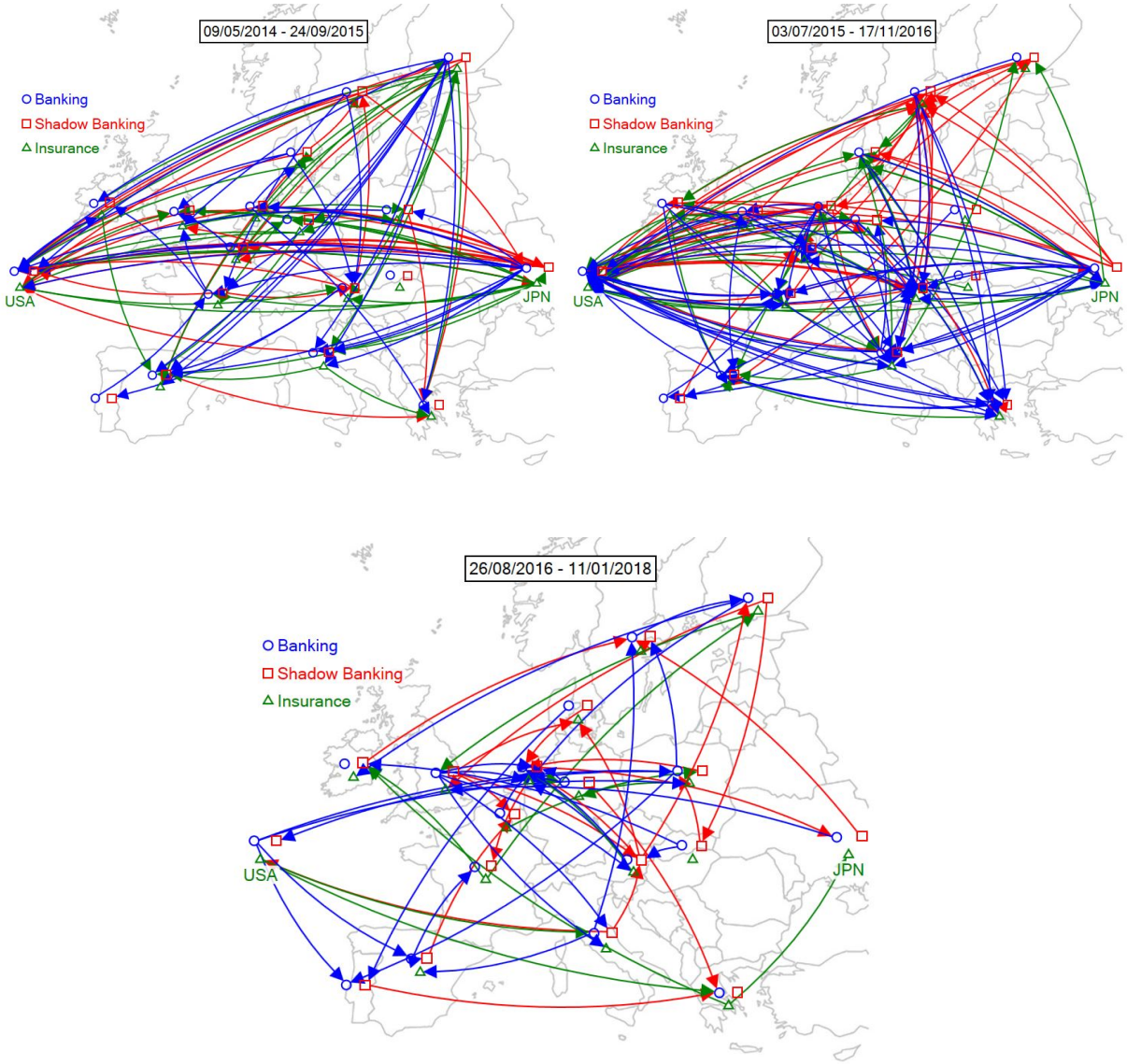

Figure 4: Temporally equidistant network snapshots during the period 1 January 2006 to 7 February 2018. Only cross-border linkages are shown for visualisation purposes.

network by adding all links in any topology and weighing the resulting edges by the number of times the link was active. The resulting network is visualised in Figure 6. In this figure, the thickest arrows (i.e. those present in the largest number of network instances) are connecting the US and Japan, the two largest countries in our sample, and for all three segments of the financial system. As this network representation focuses on synchronous links, we expect that the largest countries exhibit a common factor in their risk movements. However, this network representation cannot reveal the dynamics of the network topology. For example, it cannot answer questions such as which countries and sectors were most central in transmitting contagion to or receiving contagion from other country-sector pairs. This representation simply

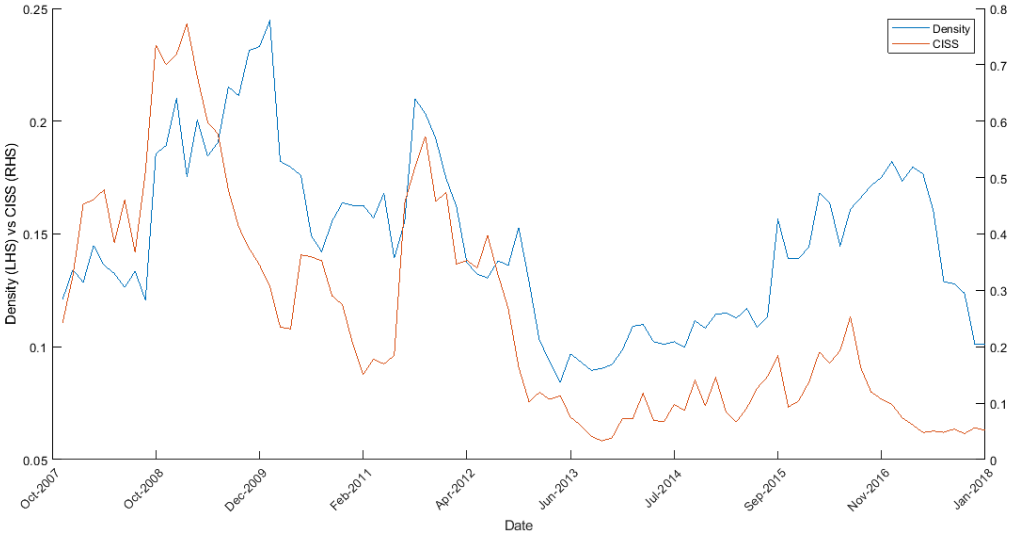

Figure 5: Density of the network vs. CISS.

confirms that, on average, the most stable co-movement of risk is the one between the financial systems of the two largest economies in our sample.

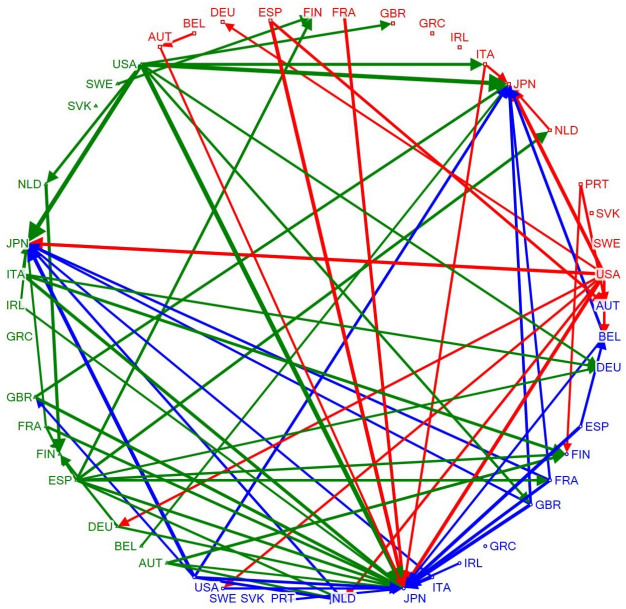

Figure 6: Aggregate network. Blue nodes and the corresponding outgoing arrows refer to banks, red to shadow banking and green to insurance. Only cross-border linkages are shown for visualisation purposes.

4.2 Standard centrality measures

We turn to the nodes of the network, i.e. the country-sector pairs, to gauge their importance in the transmission of financial stress using standard centrality measures. Figure 7 depicts the range of attained values for the out-degree metric of each country-sector pair, ordered by their median value across all network instances. As expected, the largest countries such as the US, UK, France, and countries which experienced crisis episodes, such as Spain, Italy and Greece, are all ranked high. As confirmed by Figure 8, the differences between the out-degree values across countries are clearly larger than the differences of the out-degrees across different segments of the financial sector within the same country. According to this metric, the country dimension is the main factor differentiating the importance of the various country-sector pairs, rather than the specific sector of the financial system.

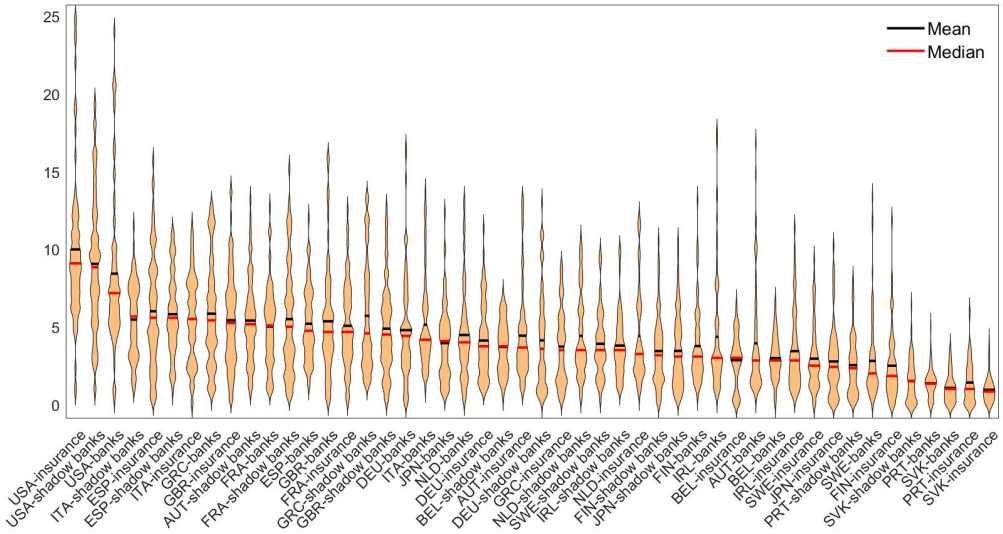

Figure 7: Range of the out-degree for each country-sector pair, ordered by their median value.

The ranking of nodes based on the reverse in-degrees metric is shown in Figure 9. The set of highest ranked countries is now different, mostly consisting of 'safe' countries such as Japan, Finland, Netherlands, Austria and Germany. As shown in Figure 10, a clearer pattern emerges when the in-degree metric is considered, in which the banking sector is the main receiver of stress.

The out- and in-degree metrics discussed so far only consider the neighbouring nodes. Therefore, these metrics do not distinguish, for example, between a source-node of contagion and a node that operated as a transmitter. Therefore, it is important to consider also the paths of

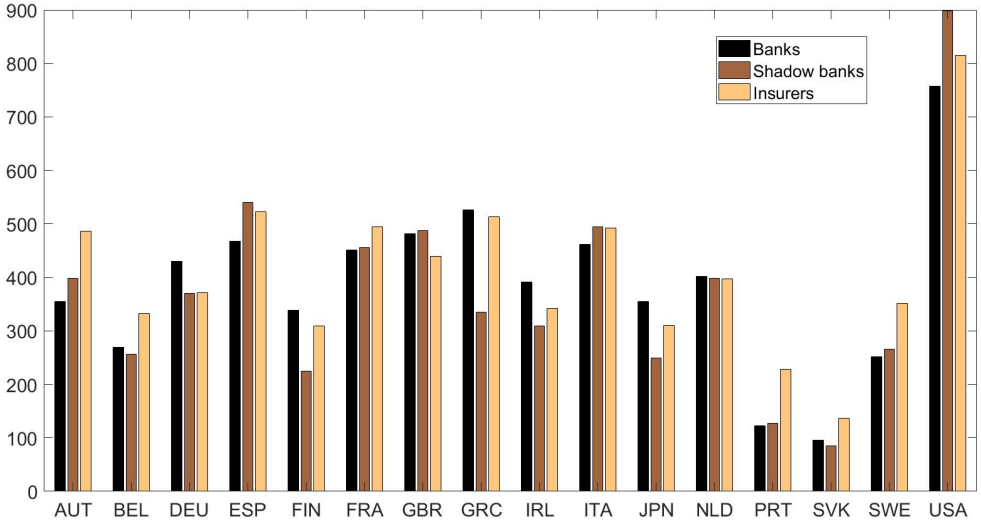

Figure 8: Total out-degree for each country-sector pair.

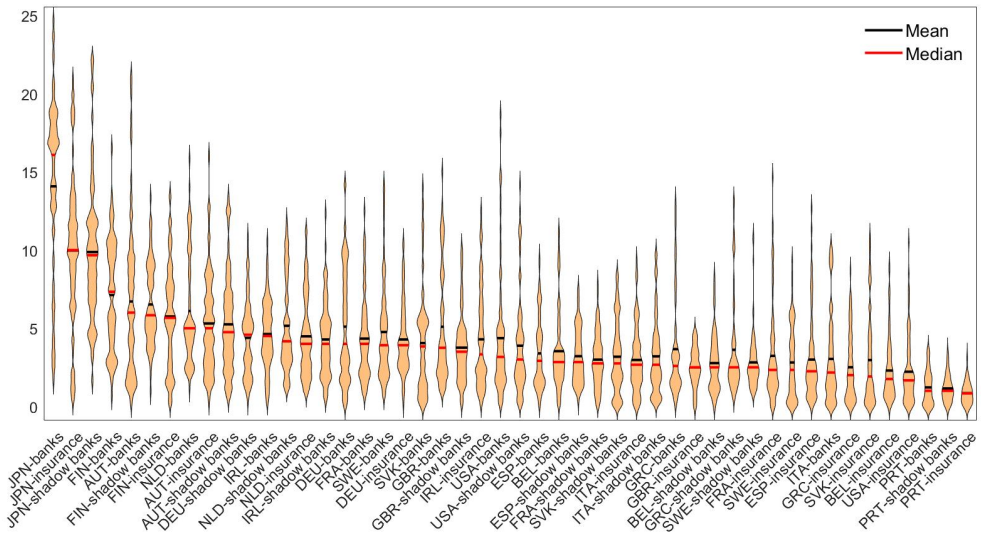

Figure 9: Ranking of the in-degree for each country-sector pair, ordered by their median value.

transmission when assessing the centrality of a country-sector pair. In Figure 11 we present the corresponding ranking of country-sector pairs based on the median value of their betweenness centrality across the network topologies. The banking sectors of the two largest countries in our sample, the US and Japan, are ranked the highest. This is a plausible result as it is to be expected that such large economies would occupy the most central role in the network, both as receivers or transmitters of shocks, to and from other countries, respectively. Following in this ranking are smaller countries such as Finland, Austria, Netherlands and Greece, followed

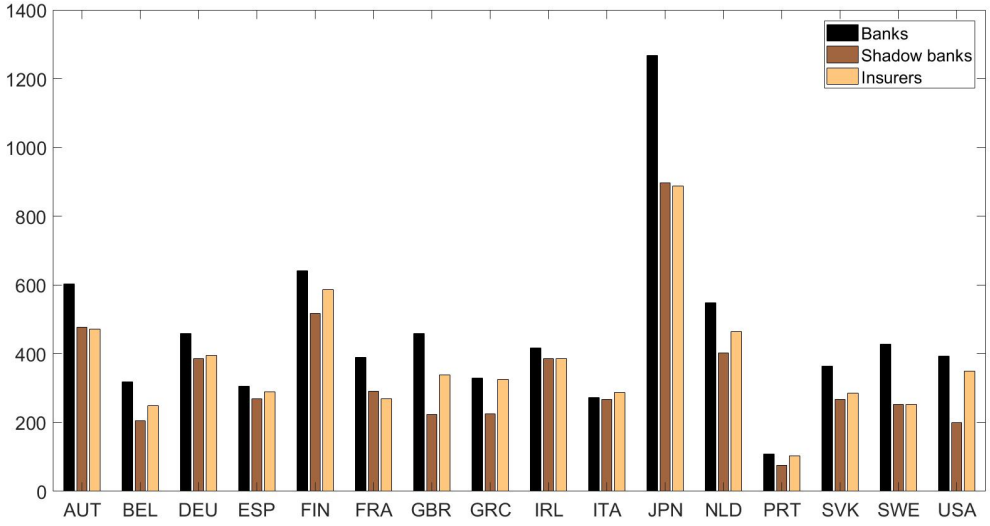

Figure 10: Total in-degree for each country-sector pair.

by Spain, Germany and France. As the betweenness centrality considers the number of shortest paths passing through a node, i.e. it does not distinguish between receivers and transmitters, this set of countries includes both crisis-hit countries and countries which may have been impacted from external shocks even if characterised by stronger fundamentals. The ranking based on betweenness centrality does not provide a clear differentiation across the sectoral dimension. However, according to this measure, the banking and shadow banking sectors seem to be more critical compared to the insurance sector, as they appear more often than the insurance sector in the highest ranks.

Figure 12 shows the corresponding ranking for the out-closeness centrality. Out-closeness centrality captures the average distance of paths leading from a node to all other nodes in the network, and for this reason it can be considered as an extended form of the out-degree measure. Large countries and crisis-hit countries exhibit the highest values of out-closeness centrality, starting with the US and Greece, and followed by the UK, Spain, France and Italy. Banks and shadow banks also dominate the highest positions when the closeness centrality is used, similarly to the case of the betweenness centrality, confirming the assessment of systemic importance for the various sectors that was provided by the betweenness centrality metric.

When the in-closeness centrality metric is used (see Figure 13), which can be considered an extension of the in-degree, a set of safe countries such as Japan, Finland, Netherlands, Austria and Germany rank the highest, similarly to the results when the in-degree was used. Banks

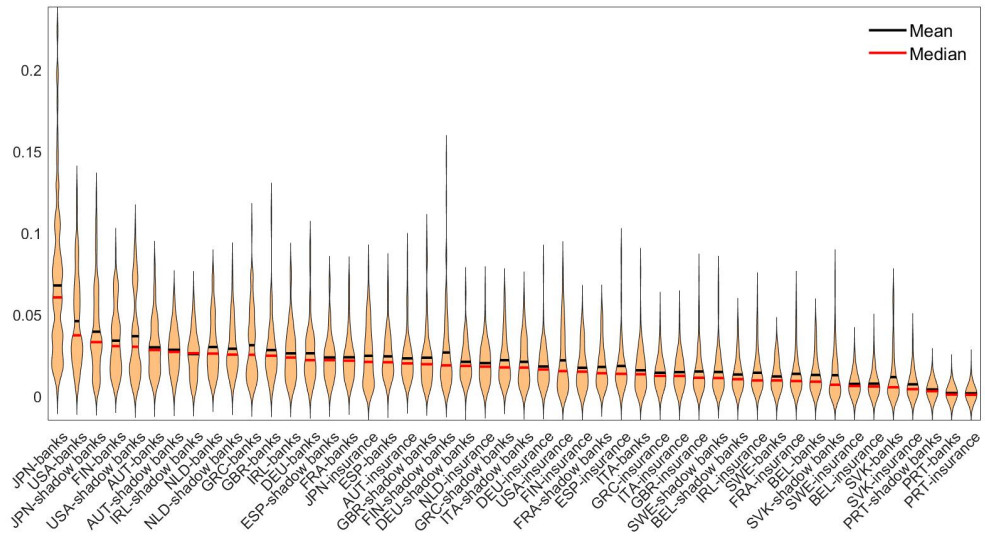

Figure 11: Ranges of the betweeness centrality of country-sector pairs, ordered by their median value.

and shadow banks tend to rank higher than insurers.

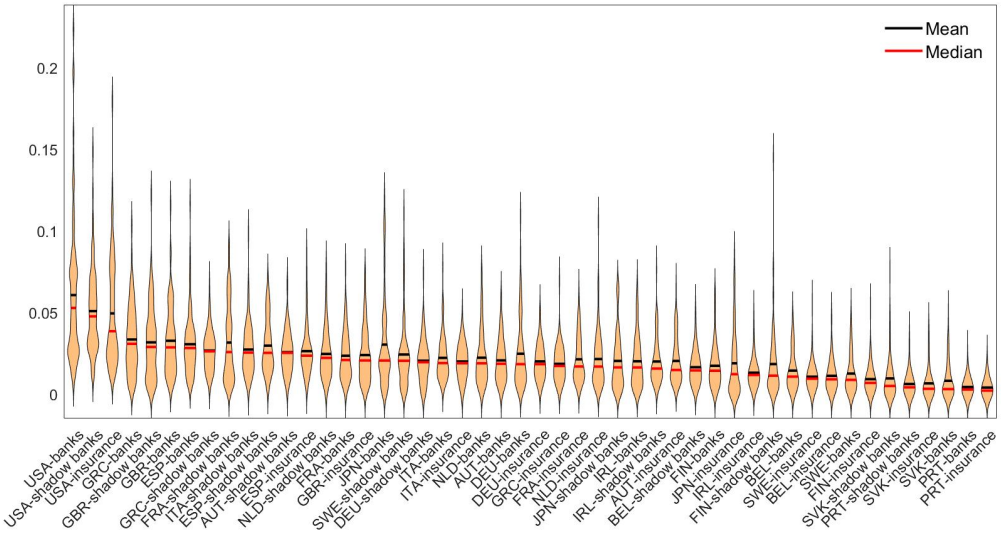

Figure 12: Ranges of the out-closeness centrality of country-sector pairs, ordered by their median value.

Overall, the results presented in this section identify a set of countries mostly consisting of large economies or crisis-stricken countries, which are identified as playing a critical role during the unfolding of contagion episodes. In addition, the results do not clearly indicate which financial segments have a more central role during financial contagion episodes, although there is some evidence that banks and shadow banks are more relevant than insurers.

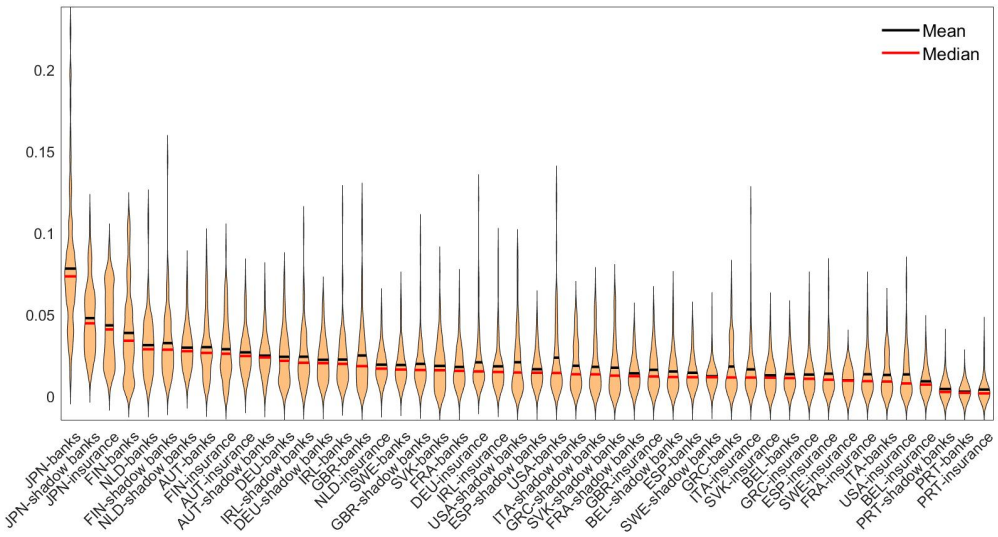

Figure 13: Ranges of the in-closeness centrality of country-sector pairs, ordered by their median value.

4.3 Higher-order centrality measures

The analysis presented in Subsection 4.2 was underpinned by static centrality measures, whereby each topology is examined separately without considering how it is related to the past or the future. As a result, the ranking of countries is specific to each instance of the network and therefore we derived an overall ranking based on the median centrality value across time for each node. As explained in Subsection 2.2, this approach can be improved upon by generalising the static network metrics to utilise the topology dynamics and examine the time-respecting paths. In this way, one does not only look e.g. whether country-sector pair x influences country-sector pair y at time t, but also whether the country-sector pair y subsequently influences another country-sector pair z in another instance of the network at time $t + \delta$. This approach considers more slowly-moving transmission channels that do not operate only through market prices.

The definition of the time scale in which we consider a subsequent link to be part of the same contagion chain is critical. In our case, we set the parameter $\delta = 1$ which corresponds to 30 observations (see Subsection 4.1). In other words, we consider the link $y \to z$ as being part of the same contagion event as $x \to y$ only if the former occurs at maximum in the next network instance after the latter, i.e. within a 30 days time window. The 30 observations window corresponds to more than one calendar month (as weekends and holidays are excluded from our sample), therefore this calibration of δ seems a plausible approach. Otherwise, there is a risk that unrelated events occurring within a time distance of two months or more would

be erroneously assigned to be parts of the same contagion phenomenon thus contaminating the contagion dynamics that we seek to capture.

Table 2 presents the ranking of the country-sector pairs obtained when the generalised second-order centralities $CC-out^{(2)}$, $CC-in^{(2)}$ and $BC^{(2)}$ are used. When the generalised closeness centrality metric $CC-out^{(2)}$ (i.e. defined based on the shortest time-respecting path from each node to all other nodes) is used, the set of countries ranked in the highest places is similar to that obtained when the corresponding static metric is used. This set comprises the same mixture of large countries, such as the US, the UK, Germany and France, and crisis-hit countries such as Spain, Greece and Italy. However, we also observe in this list a striking differentiation in the ranking of sectors, which was not present in the ranking based on the corresponding static centrality metric. The prominence of the banking sector is apparent as all nodes featuring the highest values of $CC-out^{(2)}$ refer to banks, except from the banking sectors of Slovakia, Belgium, Sweden and Portugal which are ranked lower. Shadow banks clearly represent the second most important sector and insurers seem to be the least important. Therefore, the second-order metric discriminates clearly among sectors in contrast to the static counterpart.

Table 2: Generalised centrality metrics calculated on the second-order aggregated network. 'B' refers to banks, 'Ins' to insurance firms and 'Sb' to shadow banks.

Out-closeness		**In-closeness**		**Betweenness**	
USA-B	59	GBR-B	59	JPN-B	88.9
ESP-B	59	IRL-B	58.5	BEL-Ins	59.5
GRC-B	58.5	JPN-B	58	IRL-Sb	45.1
AUT-B	58.5	AUT-B	58	FIN-B	41.6
GBR-B	58.5	FIN-B	58	GRC-B	36.5
ITA-B	58.5	NLD-B	57.5	NLD-B	24.7
DEU-B	58.5	GRC-B	57.5	DEU-B	23.5
JPN-B	58	DEU-B	57.5	JPN-Ins	22.5
IRL-B	58	AUT-Sb	57.3	IRL-B	18.4
FIN-B	57.5	FIN-Sb	57.2	BEL-B	18.3

Continued on next page

Table 2 – continued from previous page

Out-closeness		In-closeness		Betweenness	
FRA-B	57.5	IRL-Sb	57.2	AUT-B	17.4
NLD-B	57.5	JPN-Sb	57	FIN-Sb	16.7
AUT-Sb	57.3	USA-B	57	SVK-B	14.4
DEU-Sb	57	FRA-B	57	ESP-B	12.2
FRA-Sb	56.9	ESP-B	57	JPN-Sb	12.0
USA-Sb	56.9	ITA-B	57	SVK-Sb	10.5
ITA-Sb	56.9	ITA-Sb	56.8	DEU-Sb	9.9
ESP-Sb	56.7	FRA-Sb	56.7	GBR-Sb	9.7
GRC-Sb	56.6	NLD-Sb	56.6	NLD-Sb	9.5
IRL-Sb	56.3	DEU-Sb	56.4	ITA-B	9.0
FIN-Sb	56.3	USA-Sb	56.4	SWE-B	8.8
GBR-Sb	56.2	ESP-Sb	55.5	DEU-Ins	7.4
NLD-Sb	56	GBR-Sb	55	FRA-B	6.6
JPN-Sb	55.7	GRC-Sb	54.6	USA-B	6.5
FRA-Ins	53.8	GBR-Ins	53.8	FIN-Ins	5.8
GBR-Ins	53.3	AUT-Ins	53.5	AUT-Ins	5.5
SVK-B	53	IRL-Ins	53.4	SVK-Ins	5.4
ESP-Ins	52.7	FIN-Ins	53	GBR-B	5.3
AUT-Ins	52.5	JPN-Ins	52.8	ITA-Ins	5.1
DEU-Ins	52.3	ESP-Ins	52.5	FRA-Ins	5.0
FIN-Ins	52.3	SVK-B	52.5	FRA-Sb	4.6
JPN-Ins	52.3	FRA-Ins	52.2	ESP-Ins	4.5
ITA-Ins	52	DEU-Ins	52.2	GRC-Ins	4.4
NLD-Ins	52	ITA-Ins	52.2	USA-Ins	3.8
USA-Ins	51.8	GRC-Ins	52	ITA-Sb	3.6
GRC-Ins	50.8	USA-Ins	51.3	USA-Sb	3.3
IRL-Ins	50.7	BEL-B	48.5	AUT-Sb	3.0
SVK-Sb	49.5	SWE-B	48	SWE-Sb	2.8

Continued on next page

Table 2 – continued from previous page

Out-closeness		In-closeness		Betweenness	
BEL-B	49	BEL-Sb	46.7	IRL-Ins	2.8
SWE-B	48.8	NLD-Ins	46	GRC-Sb	2.5
SVK-Ins	48.5	SVK-Sb	45.8	ESP-Sb	2.3
BEL-Sb	47.5	SVK-Ins	44.3	NLD-Ins	2.1
BEL-Ins	45.5	BEL-Ins	44	GBR-Ins	2.0
SWE-Sb	45.4	SWE-Ins	42.7	PRT-Sb	1.8
SWE-Ins	43.8	SWE-Sb	37	SWE-Ins	1.8
PRT-B	37.7	PRT-B	36.2	BEL-Sb	1.1
PRT-Sb	19	PRT-Sb	17	PRT-B	0.5

Similarly, the ranking based on the second-order in-closeness centrality metric places banks at the top positions, followed by shadow banks, and with the insurance sector at lower positions. In this ranking, more shadow banks can be found in high places compared to the case of the second-order out-closeness ranking. In other words, the banking sector is more sharply ahead of the shadow banking sector in the ranking based on the second-order out-closeness compared to that based on the second-order in-closeness, reflecting the fact that the banking sector is a source or transmitter of stress with a distinctly higher frequency compared to the other sectors. The set of countries which receive the most financial stress is not much different compared to the static case, except from the fact that the UK is now found in the top position.

Finally, the ranking based on the second-order betweenness centrality also displays the same sectoral ranking as those derived from the previous two second-order metrics, with most top-ranking positions occupied by banking sectors, however it should be noted that the Belgian insurance and the Irish shadow banking sector are found in the second and third positions, respectively. In general, financial hubs such as Japan, Belgium, Ireland and the Netherlands are identified as having a prominent role as transmitters in the topology of causality networks.

To further illustrate the differences in the rankings obtained using the second-order and the static metrics, Figures 14, 15 and 16 provide the two corresponding rankings in scatterplots for the out-closeness, in-closeness and betweenness, respectively. The numbering of the rankings

starts at number 1, therefore the most systemically important nodes have a value close to 1 in at least one of the two axes. Consistently with the observations made in Subection 4.2, most network nodes are close to the 45-degrees line and most bank nodes (with blue colour) below that line. This reflects that the ranking of most countries does not change much when we switch from the static to the second-order metrics and that banks are much more clearly identified as having a critical role in contagion when the second-order metrics are used. We focus next on the cases where there is a large divergence between the ranking based on the second-order and the corresponding static centrality metric, i.e. on the nodes which are away from the 45-degrees line and are also close to the beginning of one of the two axes (i.e. they are ranked highly in one of the two alternative versions of the given metric).

The comparison of the out-closeness centralities (Fig. 14) shows that the banking sectors of crisis-hit countries, such as Italy and Ireland, and also of Germany and Austria, feature higher centrality values when the second-order metric is used. By contrast, the shadow banking sectors of the US and Japan and the insurance sector of the UK are ranked lower when the second-order out-closeness centrality is used. These differences reflect both the increased weight that the second-order metric attaches to the banking sector compared to the static metric and, in addition, the more nuanced identification of crisis-hit countries by the second-order version of the out-closeness centrality.

The same pattern is even more clearly illustrated in the ranking differences among the two versions of the in-closeness metric (Fig. 15). In this case, the banking systems of Spain, Italy and Greece are ranked higher when the second-order approach is used while at the same time the non-bank sectors of a large and two smaller but relatively safe countries (specifically, the insurance sectors of Japan, Finland and Austria) are ranked much lower.

Finally, the same pattern can be also discerned in the case of the betweenness centrality (Fig. 16). An additional element here is that also a non-bank node is classified clearly higher by the second-order metric, specifically the insurance sector of Belgium. This seems to be highly intuitive given the prominent cases of financial conglomerates with significant insurance activities in Belgium (such as Belfius/Fortis and Dexia) that came into trouble during the global financial crisis phase.

Therefore, a few general patterns emerge from the comparison of second-order and static centrality metrics. First, second-order metrics identify more clearly nodes that are known to be sources of shocks (e.g. the distress countries mentioned above) compared to the corresponding

static ones. Second-order metrics also rank much more clearly the financial segments according to their role in the transmission of stress, with banks ranked first followed by shadow banks and at lower positions the insurance sector. The degree of sectoral differentiation depends on the specific metric used but it is clearly discernible in all cases while this is not the case when the static metrics are used. Furthermore, the static centralities seem to overemphasise the role of large countries, such as the US or Japan, in the transmission of contagion. Even if these large countries participate in a large number of links, as it is clearly illustrated in the aggregate network depicted in Fig. 6, these links do not form a part of a time-respecting path through which financial stress is propagated (in contrast to the links formed by crisis-hit countries) and rather reflect the participation of large countries in relatively large number of synchronous links or paths. Therefore, the relatively higher values attained countries when static metrics are used reflect also the above average co-movement of the large countries with other countries. However, as the second-order metrics suggest, crisis-hit countries form part of contagion paths relatively more often when we consider the time series of topologies.

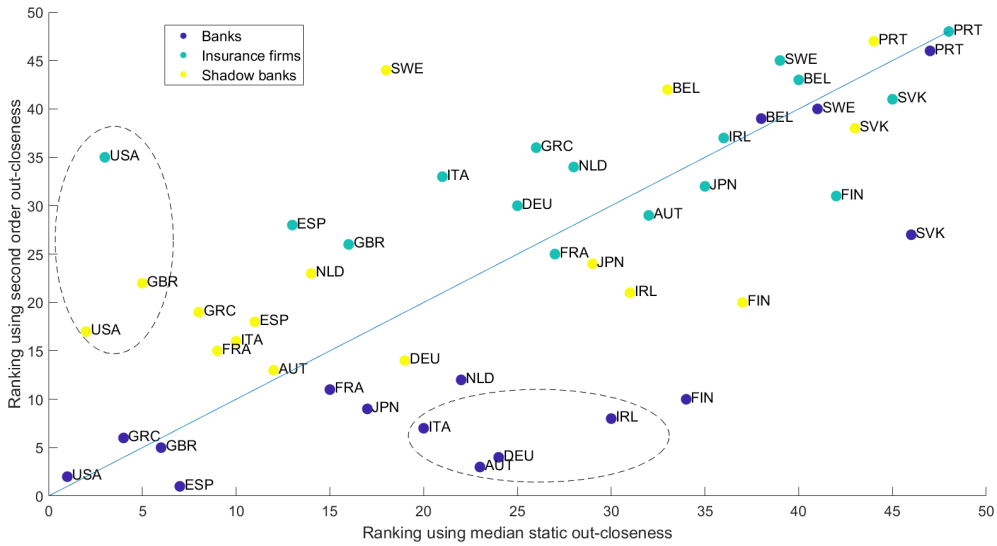

Figure 14: Static vs. 2nd order out-closeness ranking.

4.4 Cross-sectoral contagion

In this subsection we focus specifically on the sectoral dimension, aiming to understand the direction of contagion within the financial system. For this purpose we utilise both the sequence of network instances and the second-order aggregate network representation. In this investigation

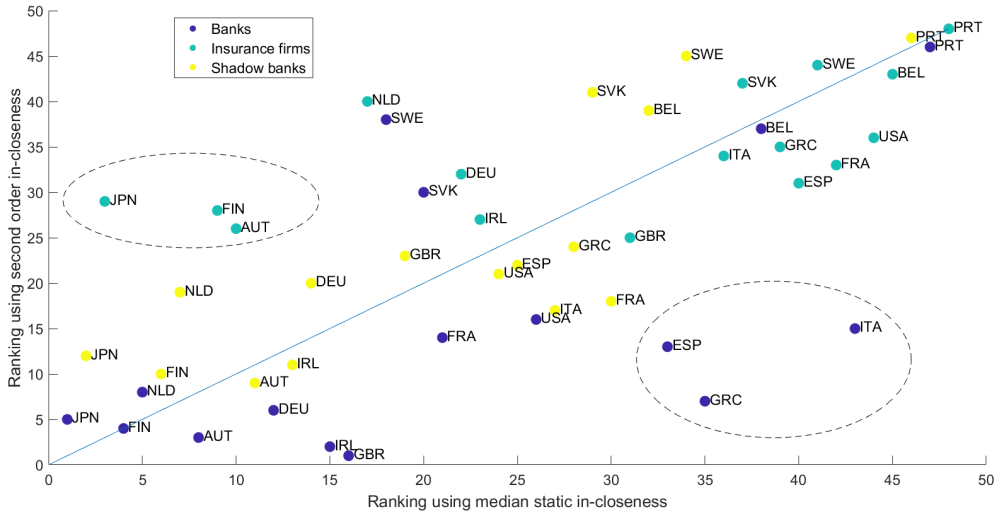

Figure 15: Static vs. 2nd order in-closeness ranking.

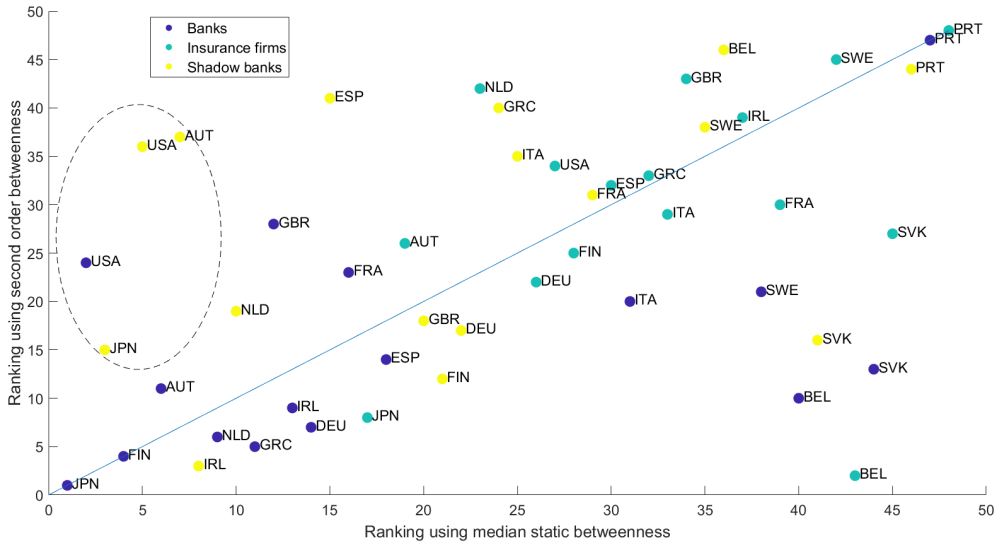

Figure 16: Static vs. 2nd order betweenness ranking.

we generally abstract from the country dimension and only distinguish between the cross- and within-country causality-in-risk paths.

First, we quantify the occurrence of each specific sectoral direction of contagion (e.g. banks → insurers). We aggregate the number of each cross-sectoral, cross-country contagion links (i.e. from country i to all other countries j, including country i) across the whole sequence of the individual network instances and plot these quantities for each direction in Figure 17.

The time series reflect similar dynamics as for the density of the entire network, displaying

peaks during the crisis periods of 2008-2009 and 2012 while the intensification of stress during 2016-2017 also emerges. Secondly, the contagion directions shadow banks → banks and banks → shadow banks are clearly the most commonly recurring. Contagion links involving insurers are less frequent. When the total number of links across time is considered, the direction shadow banks → banks occurs 6,003 times in total while the direction banks → shadow banks occurs 5,259 times.

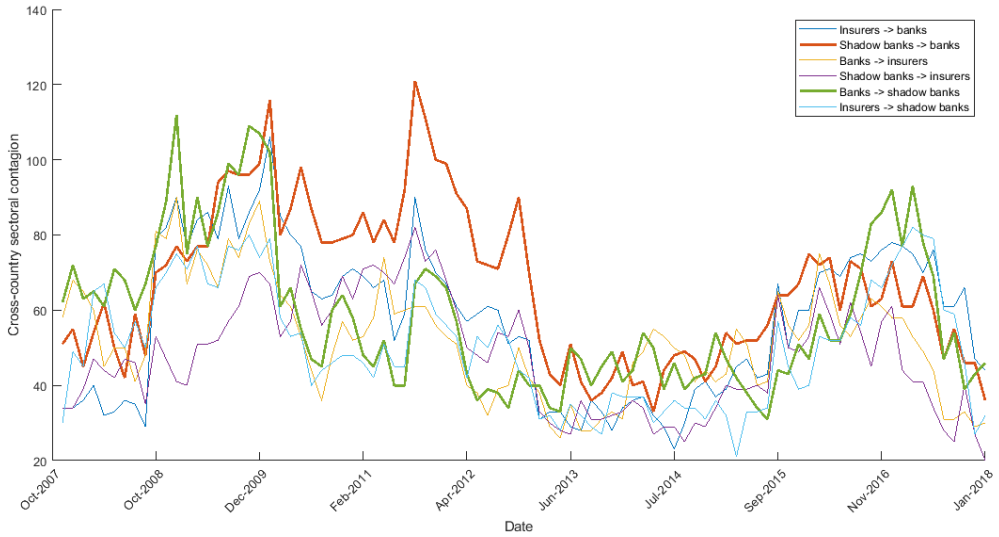

Figure 17: Cross-country sectoral contagion.

These results hold if we focus only on contagion taking place within one country. Specifically, we compute the total number of cross-sectoral, within-country (from country i to i itself, for all i) contagion links, for each specific sectoral contagion direction, again across the whole time span. We plot these quantities separately for each sectoral direction in Figure 18.

As expected, there is a lower number links in the within-country case, compared to Figure 17, as we restrict our attention only to contagion taking place within one country. The shadow banks → banks is the dominant path in this case as well. Edges with insurers appear less often also in this case. Aggregation over time confirms that the most frequently occurring links are the shadow banks → banks (occurs 360 times) and banks → shadow banks (occurs 267 times).

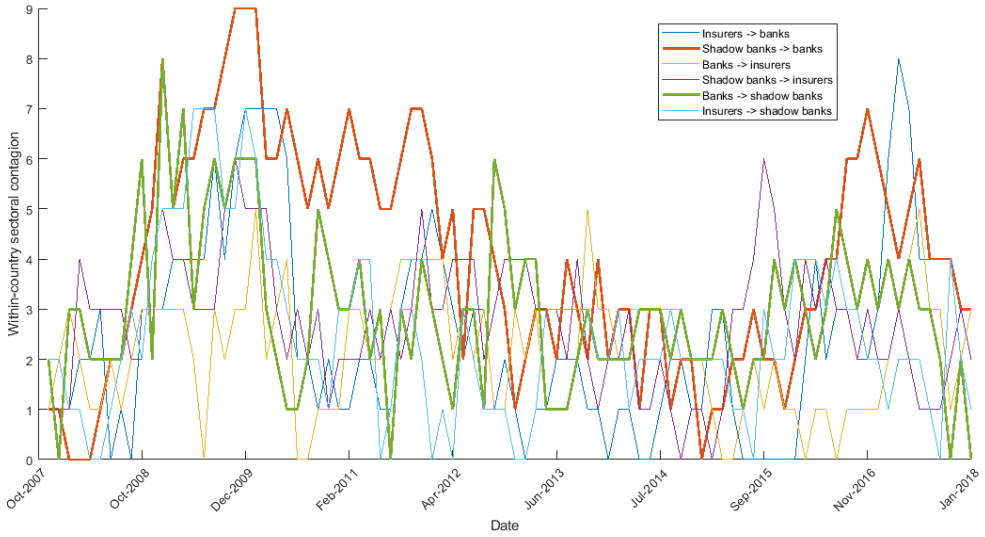

Figure 18: Within-country sectoral contagion.

Furthermore, we analyse paths of contagion episodes of length larger than one, using the second-order aggregate network. This allows us to consider paths of length two, e.g. banks → shadow banks → insurers. We use the adjacency matrix from the second-order representation of the network sequence over the whole sample period and count the frequency of occurrence for each link in that representation (which by definition corresponds to a path of length two in the temporal network representation). The results are reported in Table 3.

The contagion scenario shadow banks → banks → banks occurs more frequently than all others (in total 1,982 times), followed closely in number of occurrences by the scenario banks → banks → banks (1,937 times) and banks → shadow banks → banks (1,757 times). In comparison, contagion chains with insurers as the source of stress are found to occur much less often and the insurance sector acts mainly as a receiver (rather than the origin) of stress. Therefore, the evidence provided here points to a tight interconnectedness between the banking and the shadow banking sectors, with the insurance sector being less systemically important.

As a robustness check we examine whether these results hold during the various critical phases of the examined period, i.e. we analyse the chain of contagion events also separately for four periods: the pre-crisis period January 2006 - August 2007, the global financial crisis period August 2007 - April 2010, the European sovereign debt crisis April 2010 - July 2012 and finally the post 'whatever it takes' period July 2012 - February 2018 when sporadic and less intense crisis episodes occurred. We derive separately for each period the second-order aggregate network representation and count the frequency of occurrence of the cross-sector

contagion paths (of length two).[18] Table 4 reports the results (sorted in decreasing order, with the three largest numbers in bold).

Table 3: Chains of contagion of length two - full sample

Contagion path	Frequency
Shadow banks → banks → banks	1982
Banks → banks → banks	1937
Banks → shadow banks → banks	1757
Shadow banks → shadow banks → banks	1666
Insurers → banks → banks	1651
Banks → insurers → banks	1438
Insurers → shadow banks → banks	1415
Shadow banks → insurers → banks	1357
Insurers → insurers → banks	1090
Insurers → banks → insurers	353
Insurers → insurers → insurers	310
Shadow banks → insurers → insurers	277
Shadow banks → banks → insurers	267
Banks → insurers → insurers	245
Banks → banks → insurers	195
Insurers → shadow banks → insurers	195
Shadow banks → shadow banks → insurers	163
Shadow banks → banks → shadow banks	113
Banks → shadow banks → insurers	112
Shadow banks → insurers → shadow banks	100
Banks → banks → shadow banks	84
Shadow banks → shadow banks → shadow banks	72
Banks → insurers → shadow banks	69
Banks → shadow banks → shadow banks	49
Insurers → shadow banks → shadow banks	49
Insurers → banks → shadow banks	40
Insurers → insurers → shadow banks	23

[18] Note that this methodology implies that the sum across periods can exceed the value that is based on the whole sample.

Table 4: Chains of contagion of length two - subsamples

Contagion path	Jan06 - Aug07	Aug07 - Apr10	Apr10 - Jul12	Jul12 - Feb18
Banks → banks → banks	**298**	**737**	401	**926**
Shadow banks → banks → banks	237	**759**	**601**	**896**
Banks → shadow banks → banks	**308**	595	**429**	**889**
Insurers → banks → banks	152	**682**	390	841
Shadow banks → shadow banks → shadow banks	**276**	475	**551**	811
Insurers → shadow banks → shadow banks	252	470	380	724
Banks → insurers → banks	236	600	386	682
Shadow banks → insurers → banks	175	583	403	561
Insurers → insurers → banks	151	454	275	554
Insurers → insurers → insurers	63	83	41	162
Shadow banks → insurers → insurers	58	57	58	140
Banks → insurers → Insurers	65	50	29	120
Insurers → shadow banks → insurers	32	47	35	91
Shadow banks → shadow banks → insurers	25	34	39	77
Banks → banks → insurers	30	65	51	66
Shadow banks → insurers → shadow banks	11	14	12	65
Insurers → banks → insurers	38	164	140	58
Shadow banks → shadow banks → shadow banks	6	7	3	56
Shadow banks → banks → insurers	36	98	121	54
Banks → shadow banks → insurers	22	33	10	52
Shadow banks → banks → shadow banks	7	7	56	44
Banks → shadow banks → shadow banks	9	2	3	35
Banks → insurers → shadow banks	7	20	13	29
Insurers → shadow banks → shadow banks	7	21	2	19
Banks → banks → shadow banks	6	27	37	14
Insurers → banks → shadow banks	0	13	17	12
Insurers → insurers → shadow banks	2	5	5	11

During the pre-crisis period January 2006 - August 2007, the most frequent paths are found to be: banks → shadow banks → banks (occurring 308 times), banks → banks → banks (298 times) and shadow banks → shadow banks → shadow banks (276 times). The period of the global financial crisis August 2007 - April 2010 features the causal path shadow banks → banks → banks as the most frequent contagion chain (759 times), followed by the chain featuring solely the banking sector (737 times) and followed by insurers → banks → banks (682 times). Interestingly, this is the only period for which the insurance sector is found frequently in contagion paths also as a source. During the European sovereign debt crisis (April 2010 - July 2012), banks and shadow banks were the protagonists of contagion episodes: the path shadow banks → banks → banks occurred 601 times, the path shadow banks → shadow banks → shadow banks occurred 551 times and finally banks → shadow banks → banks is observed 429 times. Finally, during the post-2012 period (i.e. July 2012 - February 2018) contagion paths involving banks and shadow banks also dominated: banks → banks → banks (926 times), shadow banks → banks → banks (896 times) and banks → shadow banks → banks (889 times).

These results are intuitive and reflect the most well-known events that unfolded during the respective crisis episodes. For example, the global financial crisis in 2007 had its origin in the subprime market where shadow banking entities sponsored by banks repackaged subprime mortgages into securities. In addition, this period featured defaults of prominent insurance companies, leading to stress propagation more widely into the financial system; however, this was not the case in the following years when insurance companies appear to have been insulated and were not at the epicenter of other crises. In general, we confirm that the nexus between banks and shadow banks dominates (in both directions) over links involving insurers.

In addition, these results show that while both shadow banks and banks represent potential sources of contagion, the banking sector represents the main intermediary sector in the propagation of contagion. This is shown clearly in Tables 3 and 4, as the banking sector functions far more frequently as an intermediary node compared to the shadow banking and insurance sectors. This is consistent with the results discussed in Subsection 4.3 that focused on specific nodes, as the dominant position of banks derived by the second-order metrics is shown here to be due to the critical role of banks in transmitting contagion, which may have originated in other parts of the financial system, either other banks or the shadow banking sector.

5 Conclusion

The financial system has become ever more interconnected during the last decades, driven by the opening up of international trade and technological innovation including digital technology. The increasing complexity of the financial world manifests itself also in contagion phenomena which transcend the boundaries among countries and different segments of the financial system.

In this study we trace the dynamics of contagion across countries and sectors of the financial system, covering the turbulent period that started in 2007 and has continued up to 2018 with spurts of financial stress, triggered by both political and economic developments. We construct Granger causality-in-risk networks with time-varying topologies for the time span 2006-2018, based on underlying credit risk data compiled by Moody's for the banking, shadow banking and insurance sectors of 16 advanced economies. For the first time in the financial contagion literature, we apply the concepts of time-respecting paths, higher-order networks and generalised centrality measures to identify the directions through which financial stress is transmitted. The dynamics of the network density are found to reflect closely the CISS, an index of euro area financial stress, providing evidence that transmission of stress across financial entities is intensified during crisis episodes.

Our analysis points to the tight interconnectedness of the banking and shadow banking sectors during contagion episodes and the relatively lower systemic risk posed by the insurance sector. Overall, the average crisis event starts either from the banking or the shadow banking sector, while insurers are most often affected at a later stage. Specifically, based on the second-order aggregated network of causality-in-risk links, we identify episodes involving bi-directional feedback loops between banks and shadow banks as the most frequently occurring transmission paths. We also find that the insurance sector acts as a source of stress during the phase of the global financial crisis, consistently with the well-known financial troubles experienced by large insurers such as the AIG in 2008. In addition, we identify the crucial role of the banking sector as a transmitter of financial contagion. Banks are found to be in the intermediate nodes of contagion paths much more often then either shadow banks or insurance firms.

In general, we find that it is crucial to move beyond static network analysis in order to capture the importance of the various segments of the financial sector and the different countries during crisis episodes. The generalised centrality metrics, constructed using the second-order network representation, identify more clearly than the corresponding static measures the bank-

ing and shadow banking sectors as the primary financial segments where financial contagion takes place. In addition, the generalised centrality metrics identify the insurance sector as a critical financial segment in a few cases that correspond well to known cases of financial distress in that sector. In addition, second-order centrality metrics provide a much clearer characterization of countries experiencing distress, such as Spain, Italy and Greece, as critical nodes during crisis episodes.

The evidence of financial contagion transmitted across financial sectors could inform the design of macroprudential policy and banks' supervision. Stress tests to assess banks' solvency should not neglect the second-order effects of an initial shock which could be realised due to the links of banks to the rest of the financial system (Baranova et al. (2017)). The macroprudential policy stance should be consistent across the segments of the financial system, otherwise it may be less effective and could promote the amplification of shocks, a result which is consistent with Feve et al. (2019).

Our analysis is statistical in nature, and we do not seek to distinguish transmissions channels operating during crises, e.g. due to direct exposures and indirect exposures. This extension would be of great interest for future research and could also exploit temporal node centrality concepts to analyse dynamic networks, as done in this paper. Also, in our non-parametric setting, we robustify the Granger causality-in-distribution test ex-post by integrating over the kernels and truncation parameters. An alternative approach on how to deal with biases in network metrics due to edge estimation and measurement errors could be the de-noising procedure proposed by Billio et al. (2021b). Finally, it is interesting to apply our framework when comparing estimated versus physical data, following the taxonomy of "informational" versus "portfolio/balance sheet-related" contagion (Allen et al. (2011)) or between "correlation/dependence" versus "physical" contagion (Brunetti et al. (2019)). Following this approach it could be explored whether during crises "informational" contagion increases while physical interconnections (e.g. interbank lending) simultaneously become less dense (Brunetti et al. (2019)). We leave these extensions to future research.

Appendix A. VaR estimation

To perform the Granger causality-in-distribution test we need to estimate the VaR levels so as to identify tail events for each node, i.e. a country-sector pair, of the network. Therefore, we

employ customized parametric models which are chosen by means of model selection criteria. Specifically, we estimate GARCH models (Bollersev (1986)) for each country-sector pair in order to account for heteroscedasticity in the EDFs that could bias tests of contagion (Candelon and Tokpavi (2016), p. 25, and Forbes and Rigobon (2002))[19]. In particular, we estimate a battery of $AR(n) - GARCH(q, s)$ models as follows:

$$y_{ij,t} = \mu_{ij} + \sum_{m=1}^{n} \rho_m y_{ij,t-m} + \sum_{k=1}^{4} \theta_k \mathbb{1}_{k,ij,t} + \epsilon_{ij,t} \tag{12}$$

$$\epsilon_{ij,t} = u_{ij,t}\sigma_{ij,t} \tag{13}$$

$$\sigma^2_{ij,t} = \omega_{ij} + \sum_{p=1}^{q} \beta_p \epsilon^2_{ij,t-p} + \sum_{r=1}^{s} \gamma_r \sigma^2_{ij,t-r} \tag{14}$$

where $y_{ij,t}$ represents changes of EDFs in sector i and country j on day t and is a function of a constant[20] μ_{ij}, its own lagged value(s) $y_{ij,t-m}$, a set of indicator variables $\mathbb{1}_{k,ij,t}$ to allow for structural breaks in means across the four main phases of the period under investigation (see Section 3)[21] and $u_{ij,t}$ is i.i.d. noise with zero mean and unit variance. The conditional variance $\sigma^2_{ij,t}$ is a function of a constant ω_{ij} and depends on past shocks $\epsilon^2_{ij,t-p}$ and its lagged values $\sigma^2_{ij,t-r}$. We define the model space by setting $n \in \{0, 1\}$ and $q, s \in \{1, 2, 3\}$. ρ_m, θ_k, β_p and γ_r are parameters. We choose the model specification based on the AIC.[22]

Model estimation is performed via quasi-maximum likelihood allowing the errors $u_{ij,t}$ to be either Gaussian or follow a t distribution. The latter option accommodates heavy-tailed EDF changes. To ensure plausible estimations, e.g. which do not exhibit explosive behaviour, we employ restrictions on the coefficients. Specifically, we impose positive values for the ARCH, GARCH and constant coefficients while constraining the sums of GARCH coefficients to ensure convergence of the conditional variance to a positive value, i.e. $\sum_{p=1}^{q} \beta_p + \sum_{r=1}^{s} \gamma_r \leq 1$. Finally, we use Huber-White (or sandwich) robust variance estimates.

We consider the set $A \in \{\alpha_1, \alpha_2, \alpha_3\}$ of risk levels $\alpha_1 = 90\%$, $\alpha_2 = 95\%$ and $\alpha_3 = 100\%$.

[19] Forbes and Rigobon (2002) frame the discussion in terms of the bias that heteroscedasticity causes towards the estimation of cross-correlation between markets.

[20] We use constants unlike e.g. Candelon and Tokpavi (2016)), as we do not model equity returns that have zero mean changes but EDFs where the expected value is not zero.

[21] The results we obtain remain qualitatively similar when excluding the indicator variables.

[22] We aim at taking into account all possible transmission channels, therefore we do not condition on variables besides lagged EDFs so that the derived VaRs contain all information explained by EDFs past values, given the conditional volatility at each point in time.

The VaRs, on which the causality tests are performed, are then obtained as

$$\hat{VaR}_{ij,t,s} = \hat{\mu}_{ij} + \sum_{m=0}^{n} \hat{\rho}_m y_{ij,t-m} + \hat{\sigma}_{ij,t} q(\hat{u}_{ij,t}, \alpha_s) \tag{15}$$

where $s \in \{1, 2, 3\}$, $\hat{\sigma}_{ij,t}$ is the fitted volatility at time t and $q(\hat{u}_{ij,t}, \alpha_s)$ is the sample α_s-quantile of the standardized residuals $\hat{u}_{ij,t}$.

References

Acemoglu, D., A. Ozdaglar, and A. Tahbaz-Salehi (2015). Systemic risk and financial stability in financial networks. *American Economic Review 105*(2), 564–608.

Allen, F. and E. Carletti (2006). Credit risk transfer and contagion. *Journal of Monetary Economics 53*, 89–111.

Allen, F., E. Carletti, J. P. Krahnen, and M. Tyrell (2011). *Liquidity and crises*. Oxford University Press.

Baranova, Y., J. Coen, L. P., J. Noss, and L. Silvestri (2017). Simulating stress across the financial system: the resilience of corporate bond markets and the role of investment funds.

Billio, M., R. Casarin, M. Costola, and M. Iacopini (2021a). Covid-19 spreading in financial networks: a semiparametric matrix regression model. *Working Papers 2021:05, Department of Economics, Universit of Venice "'Ca Foscari"*.

Billio, M., R. Casarin, M. Costola, and M. Iacopini (2021b). A matrix variate t model for networks. *Frontiers in Artificial Intelligence 4*.

Billio, M., R. Casarin, M. Iacopini, and S. Kaufmann (2017). Bayesian dynamic tensor regression. *Arxiv*.

Billio, M., L. Fratarollo, H. Gatfaoui, and P. Peretti (2016). Clustering in dynamic causal networks as a measure of systemic risk on the euro zone. *SYRTO Working Paper Series* (3).

Billio, M., M. Getmansky, A. Lo, and L. Pelizzon (2012). Econometric measures of connectedness and systemic risk in the finance and insurance sectors. *Journal of Financial Economics 104*, 535–559.

Blasques, F., S. Koopman, L. A., and S. J. (2016). Spillover dynamics for systemic risk measurement using spatial financial time series models. *Journal of Econometrics 195*, 211–223.

Bollersev, T. (1986). Generalized autoregressive conditional heteroskedasticity. *Journal of Econometrics 31*(3), 307–327.

Bonaccolto, G., M. Caporin, and R. Panzica (2019). Estimation and model-based combination of causality networks among large US banks and insurance companies. *Journal of Empirical Finance 54*, 1–21.

Bongaerts, D., F. De Jong, and J. Driessen (2011). Derivative pricing with liquidity risk: Theory and evidence from the credit default swap market. *Journal of Finance 66*(1), 203–240.

Brownlees, C., C. Hans, and E. Nualart (2021). Bank credit risk networks: Evidence from the eurozone. *Journal of Monetary Economics 117*, 585–599.

Brunetti, C., J. Harris, S. Mankad, and G. Michailidis (2019). Interconnectedness in the interbank market. *Journal of Financial Economics 133*, 520–538.

Candelon, B. and S. Tokpavi (2016). A nonparametric test for Granger causality in distribution with application to financial contagion. *Journal of Business & Economic Statistics 34*(2), 240–253.

Caporin, M., L. Pelizzon, F. Ravazzolo, and R. Rigobon (2018). Measuring sovereign contagion in Europe. *Journal of Financial Stability 34*, 150–181.

Chen, H., D. Cummins, K. Viswanathan, and M. Weiss (2014). Systemic risk and the interconnectedness between banks and insurers: An econometric analysis. *Journal of Risk and Insurance 81*(3), 623–652.

Chinazzi, M., G. Fagioli, J. Reyes, and S. Schiavo (2013). Post-mortem examination of the international financial network. *Journal of Economic Dynamics and Control 37*, 1692–1713.

Clayes, P. and B. Vasicek (2014). Measuring bilateral spillover and testing contagion on sovereign bond markets in Europe. *Journal of Banking and Finance 46*, 151–165.

Corsi, F., F. Lillo, D. Pirino, and L. Trapin (2018). Measuring the propagation of financial distress with Granger-causality tail risk networks. *Journal of Financial Stability 38*, 18–36.

Danielsson, J. Song Sin, H. and J. Zigrand (2013). Endogenous and systemic risk. In J. G. Haubrich and A. Lo (Eds.), *Quantifying Systemic Risk*, pp. 73–94. University of Chicago Press.

de Groen, W. P. (2011). A closer look at Dexia: The case of misleading capital ratios. *CEPS Commentary*.

De Santis, R. and S. Zimic (2017). Spillovers among sovereign debt markets: Identification through absolute magnitude restrictions. *Journal of Applied Econometrics 33*, 727–747.

Eichler, M. (2007). Granger causality and path diagrams for multivariate time series. *Journal of Econometrics 137*, 334–353.

Fernandez-Rodriguez, M., M. Gomez-Puig, and S. Sosvilla-Rivero (2016). Using connectedness analysis to assess financial stress transmission in EMU sovereign bond market volatility. *Journal of International Financial Markets, Institutions and Money 43*, 126–145.

Feve, P., A. Moura, and O. Pierrard (2019). Shadow banking and financial regulation: A small-scale DSGE perspective. *Journal of Economic Dynamics and Control 101*, 130–144.

Forbes, K. and R. Rigobon (2002). No contagion, only interdependence: measuring stock market comovements. *Journal of Finance 57*(5), 2223–2261.

Gai, P., A. Haldane, and S. Kapadia (2011). Complexity, concentration and contagion. *Journal of Monetary Economics 58*, 453–470.

Gertler, M., N. Kiyotaki, and A. Prestipino (2016). Wholesale banking and bank runs in macroeconomic modelling of financial crises. In J. B. Taylor and H. Uhling (Eds.), *Handbook of Macroeconomics*, pp. 1346–1423. Elsevier.

Gorbanyov, M. and T. Tressel (2016). Luxembourg: Selected issues. *IMF Country Report*.

Holló, D., M. Kremer, and M. Lo Duca (2012). CISS - a composite indicator of systemic stress in the financial system. *ECB Working Paper Series* (1426).

Hong, Y., Y. Liu, and S. Wang (2009). Granger causality in risk and detection of extreme risk spillover between financial markets. *Journal of Econometrics 150*(2), 271–287.

Hsiao, C. (1982). Autoregressive modeling and causal ordering of economic variables. *Journal of Economic Dynamics and Control 4*, 243–259.

Jarrow, R. (2012). Problems with using CDS to infer default probabilities. *Journal of Fixed Income 21*(4), 6–12.

Langfield, S., Z. Liu, and O. T. (2014). Mapping the UK interbank system. *Journal of Banking and Finance 45*, 288–303.

Lee, T. and W. Yang (2014). Granger-causality in quantiles between financial markets: Using copula approach. *International Review of Financial Analysis 33*, 70–78.

McDonald, R. and A. Paulson (2015). AIG in hindsight. *Journal of Economic Perspectives 29*(2), 81–106.

Meeks, R., B. Nelson, and P. Alessandri (2017). Shadow banks and macroeconomic instability. *Journal of Money, Credit and Banking 49*(7), 1483–1516.

Podlich, N. and M. Wedow (2014). Cross-border financial contagion to Germany: How important are OTC dealers? *International Review of Financial Analysis 33*, 1–9.

Rosvall, M., A. Esquivel, A. Lancichinetti, J. West, and R. Lambiotte (2014). Memory in network flows and its effects on spreading dynamics and community detection. *Nature Communications 5*.

Scholtes, I., N. Wider, and A. Garas (2016). Higher order aggregate networks in the analysis of temporal networks: path structures and centralities. *European Physical Journal B 89*(61), 1–15.

Scholtes, I., N. Wider, R. Pfitzner, A. Garas, C. Tessone, and F. Schweitzer (2014). Causality-driven slow-down and speed-up of diffusion in non-Markovian temporal networks. *Nature Communications 5*.

Schwaab, B., S. Koopman, and A. Lucas (2017). Global credit risk: World, country and industry factors. *Journal of Applied Econometrics 32*, 296–317.

Shin, Y. (2009). Reflections on Northern Rock: The bank run that heralded the global financial crisis. *Journal of Economic Perspectives 23*(1), 101–119.

Tang, D. and H. Yan (2010). Market conditions, default risk and credit spreads. *Journal of Banking and Finance 34*(4), 743–753.

Tonzer, L. (2015). Cross-border interbank networks, banking risk and contagion. *Journal of Financial Stability 18*, 19–32.

Wang, G., C. Xie, K. He, and E. Stanley (2017). Extreme risk spillover network: Application to financial institutions. *Quantitative Finance 17*(9), 1417–1433.

Acknowledgements

We thank Stefano Battiston, Anthony Brassil, Adrian Carro, Serafin Martinez Jaramillo, Cosimo Pancaro, Matthias Sydow and Loriana Pelizzon for helpful comments and suggestions. Moreover, we thank the participants of the 2021 WEHIA Conference, the 2021 CEMLA conference and the 2021 RiskLab/BoF/ESRB Conference on Systemic Risk Analytics. The views expressed in this paper are those of the authors and do not necessarily reflect those of the European Central Bank.

Fabio Franch
European Central Bank, Frankfurt am Main, Germany; email: fabio.franch@ecb.europa.eu

Luca Nocciola
European Central Bank, Frankfurt am Main, Germany; email: luca.nocciola@ecb.europa.eu

Angelos Vouldis
European Central Bank, Frankfurt am Main, Germany; email: angelos.vouldis@ecb.europa.eu

Postal address 60640 Frankfurt am Main, Germany
Telephone +49 69 1344 0
Website www.ecb.europa.eu

PDF ISBN 978-92-899-5116-6 ISSN 1725-2806 doi:10.2866/760555 QB-AR-22-032-EN-N